Chapter 4

Post-combustion CO_2 absorption-desorption performance of novel aqueous binary amine blend of Hexamethylenediamine (HMDA) and 2-Dimethylaminoethanol (DMAE)

Abstract

In this investigation, a novel aqueous Hexamethylenediamine (HMDA) and 2-Dimethylaminoethanol (DMAE) amine blend was made to capture CO_2, which would strongly contribute towards net-zero emission. The capability of the novel amine blend was investigated by conducting CO_2 absorption and desorption experiments. The major research findings were equilibrium CO_2 loading (α), cyclic capacity, heat duty, regeneration efficiency, CO_2 absorption and desorption rate, pH, density, ^{13}C NMR and FTIR characterization, process optimization, and toxicity assessment. CO_2 absorption experimental operating conditions: temperature (T) = 298.15–333.15 K, CO_2 partial pressure (P_{CO2}) = 10.13–25.33 kPa, mole fraction of HMDA (m_{HMDA}) = 0.05–0.20, and solution concentration (C) = 1–3 mol/L. The optimum equilibrium CO_2 loading was found to be 1.2174 mol CO_2/mol amine at T = 298.15 K, P_{CO2} = 25.33 kPa, m_{HMDA} = 0.20, and C = 1 mol/L. Similarly, desorption experiments were performed at constant T = 393.15 K and P_{CO2} = 25.33 kPa. For C = 3 mol/L, cyclic capacity was 1.5951 mol CO_2/L solution, which was 61.77 % higher than the benchmark 30 wt% monoethanolamine (MEA). The heat duty

and regeneration efficiency for 3 mol/L solution were calculated to be 131.24 kJ/mol CO_2 and 60.47 %, respectively. The novel amine blend's heat of CO_2 absorption was calculated to be -75.50 kJ/mol. Response surface methodology (RSM) was used for modeling and optimization: $\alpha_{optimum}$ = 1.04583 mol CO_2/mol amine at T = 306.90 K, P_{CO2} = 21.53 kPa, m_{HMDA} = 0.16 and C = 1.5 mol/L.

4.1 Introduction

Climate change is a momentous worldwide concern in the present scenario, and this is due to the emission of a tremendous volume of carbon dioxide (CO_2) in the environment because of industrialization and various activities of human beings [1-11]. Agricultural sectors, power sectors, transportation sectors, petroleum and petrochemical sectors, and various chemical and non-chemical allied industries are some of the major contributors to CO_2 emissions [12-18]. The statistical data of CO_2 emissions by major industrial sectors in the United States in 2020 is shown in Table B1 of Chapter 1. Ocean acidification, increasing earth's temperature, wildlife disruption, human health issues, natural calamities, etc., are some of the major concerns of CO_2 emission [19-24]. Due to the adverse impacts of CO_2 emissions, almost every country has started focusing on carbon neutrality. Many countries around the world are aiming to meet the carbon neutrality criteria by 2050–2070. It can be achieved by implementing net-zero CO_2 emissions from every sector that is the prime CO_2 emission source. At the 26th session of the Conference of Parties (COP–26) held in Scotland, United Kingdom, in 2021, developing countries such as India pledged to achieve carbon neutrality by 2070. At COP–26, India presented its five major climate actions, with the target of achieving 500 GW of non-fossil fuel related energy production, 50 % of energy requirements relying on renewable energy resources, one billion tonnes of

projected CO_2 emission reduction, and a 45 % reduction in the economy's carbon intensity by 2030.

Carbon capture, utilization, and storage (CCUS) is mainly helpful for attaining scenarios like net-zero CO_2 emissions. Pre-combustion, post-combustion, and oxy-combustion are the three main techniques of CO_2 capture [1,7,25-29]. Post-combustion is a highly developed and reliable technique, whereas oxy-combustion is still in its early stages [30-33]. Oxy-combustion technique has some major advantages of high CO_2 capture efficiency (i.e., 80–98 %), no chemical requirement, economical operation, least pollutant emissions, and its construction is simple [3,8]. Therefore, oxy-fuel combustion could be a commendable option in the upcoming future. Figure 1.4 of Chapter 1 is the process diagram of the oxy-combustion technique implemented in thermal power plants. The CO_2 capture techniques can be implemented by adopting any of the CO_2 capture methodologies, i.e., absorption, adsorption, membrane technology, cryogenic separation, chemical looping combustion (CLC), and microalgae process [3,34-36]. Capture of CO_2 through amine scrubbing is one of the most traditional solutions for achieving carbon neutrality. Some of the very popular conventional amines for capturing CO_2 are primary amine: Monoethanolamine (MEA), secondary amine: Diethanolamine (DEA), tertiary amine: Methyldiethanolamine (MDEA), sterically hindered amine: 2-Amino-2-methyl-1-propanol (AMP), and cyclic amine: Piperazine (PZ) [1-3,15,29,31,37,38]. Amongst all these conventional amines, MEA with 30 wt% composition has been regarded as benchmark because of its high reactivity towards CO_2, commendable absorption capacity, good solubility, economical price, etc. [3,6,7,11,24,37,39]. However, the biggest drawback of MEA is its high viscosity and elevated regeneration energy demand ($\approx$ 3.7 GJ/ton CO_2)

[3,7,20,23,32,40,41]. The CO_2 chemical reaction with the primary and secondary amines (i.e., activators) produces carbamates, while tertiary amines (i.e., promoters) form bicarbonates in reaction with CO_2 [27,38,42]. The heat of absorption (ΔH_{abs}) of these primary and secondary amines is greater ($\Delta H_{abs} \approx 80$ kJ/mol CO_2) than tertiary amine ($\Delta H_{abs} \approx 60$ kJ/mol CO_2), resulting in higher regeneration costs [1,2]. According to the structure, the hydrogen atoms in tertiary amines are not directly attached to the nitrogen atoms as in the case of activators [43]. Therefore, carbamation reaction is impossible, but only CO_2 hydrolysis reaction is feasible in tertiary amines. Amine blending is a fascinating task that improves the performance of CO_2 capture loading and reduces regeneration energy demand [6,12,31,44]. Different classes of amines can be blended so that the disadvantage of one amine is balanced by the benefit of another [17,45]. Primary amine + tertiary amine, secondary amine + tertiary amine, and primary amine + hindered amine are some examples of amine blend preparation. Few of those amine blends show biphasic behavior after successful CO_2 absorption, and they have the advantage of reduced regeneration energy as juxtaposed to MEA.

Hexamethylenediamine (HMDA) is a diamine containing two primary amino groups present in its chemical structure, and these amino groups are separated by six carbon atoms [12,15,37,42,46-48]. When two amino groups go apart, a situation of decreasing electronic influence between them exists, causing increasing CO_2 absorption capacity. HMDA exhibits a high partial atomic charge on its nitrogen atom, making it better than conventional amines [49]. HMDA provides a high CO_2 absorption rate, high equilibrium CO_2 loading, is highly miscible with water, has elevated boiling point, is less volatile, and is less corrosive as compared with conventional Monoethanolamine (MEA)

[15,29,42,47,49-51]. Hadri et al. [46] conducted a screening test on 30 different aqueous amines comprising linear amines, non-linear amines, sterically hindered amines, and polyamines to judge CO_2 loading and reaction kinetics of such amines. Amongst all 30 amines, HMDA showed a maximum equilibrium CO_2 loading of 1.35 mol CO_2/mol amine, whereas Triethanolamine (TEA) resulted in the least equilibrium CO_2 loading of 0.39 mol CO_2/mol amine. Kim et al. [29] investigated the CO_2 capture behavior of some selected aliphatic diamines, i.e., PZ, 2-Methylpiperazine (2-MPZ), homopiperazine (HomoPZ), and HMDA. They concluded that HMDA acquires two amine groups that are available in its molecular structure, and its theoretical CO_2 loading can reach up to 1 mol CO_2/mol amine. However, this theoretical CO_2 loading value may change according to the experiment's working conditions and the molecular structure of amine. Gao et al. [19] investigated the CO_2 capture behavior of seven different polyamines regarding reaction rate and absorption heat. Their experimental study concluded that HMDA required maximum time to attain the CO_2-saturated equilibrium condition, initial desorption rate was slowest, and its heat of CO_2 absorption was also maximum (i.e., ΔH_{abs} = 92.22 kJ/mol) amongst all of the tested polyamines. However, the equilibrium CO_2 loading was maximum (i.e., 1.257 mol CO_2/mol amine) and acquired the least cyclic capacity.

2-Dimethylaminoethanol (DMAE) is a tertiary amine containing 2 methyl groups attached to nitrogen atoms and 1 hydroxyethyl group present in its molecular structure [43,52]. It is chemically synthesized by adding an equal percentage of ethylene oxide and dimethylamine. Amine blends of DMAE are becoming popular nowadays in CO_2 capture since DMAE is a novel amine that is obtained from renewable energy resources, which is replacing most conventional tertiary amines due to its superior behavior [1,45,53]. High

equilibrium CO_2 loading, good degradation resistance, low viscosity, fabulous thermal stability, and more pK_a value are the major advantages of DMAE. The majority of the literature also reported that DMAE also offered excellent absorption and desorption rate, low regeneration energy demand, low heat of CO_2 absorption (ΔH_{abs} < 70 kJ/mol), and low desorption enthalpy than conventional MEA [40,45,54-60]. Buvik et al. [61], in their investigation, selected 19 different amines and performed oxidative degradation, thermal degradation, and biodegradation tests. Loss of alkalinity correlated with the oxidative degradation of specific amine. Based on experimental results, they concluded that every tertiary amine tolerates high oxidation. DMAE outperformed all other amines by having the lowest amine loss of 4 %, being thermally stable, and being highly biodegradable. Brúder et al. [62] prepared two amine blends of DMAE (3M) + 3-methylaminopropylamine (MAPA) (2M) and DMAE (5M) + MAPA (1M) for screening and VLE equilibrium measurement. They reported that their amine blends did not show solid precipitation while loading CO_2. According to the commendable properties of HMDA and DMAE, a novel aqueous HMDA+DMAE amine blend can be prepared to investigate CO_2 absorption and desorption behavior. CO_2 capture investigation on blending HMDA with other amines is limited in the open literature, and according to the research, no information has been found for the aqueous amine blend of HMDA+DMAE till date. Therefore, the aqueous HMDA+DMAE amine blend is novel, and this is the first time anyone has worked on this amine blend to the best of our knowledge.

Intermediate complexes of HMDA, DMAE, carbamate (H_2NCOO^-), bicarbonate (HCO_3^-), and carbonate (CO_3^{2-}) were formed on CO_2 loading. Characterization techniques such as ^{13}C nuclear magnetic resonance (NMR) and Fourier transform infrared (FTIR)

spectroscopy analyses benefitted in authenticating such intermediate complexes [2,17,29,36,40,63-67]. When analyzing the performance of any amine blend, heat duty, regeneration efficiency, CO_2 absorption and desorption rates are always considered. The alkalinity of amine blend samples is always checked in terms of solution pH, and this value of pH gives information about the loading of CO_2 in the amine solution [12]. Response surface methodology (RSM) is a chemometric method that finds its application in every industry for optimization, modeling, and prediction, which is becoming very popular nowadays [1,2,68-71]. The RSM software designs the experimental run set according to the operating conditions and provides the best optimum result. In this approach, software develops a modeling equation correlating the response with independent variables. Central composite design (CCD), Box-Behnken design (BBD), one-factor design, optimal design, user-defined design, and historical data design are some of the very famous designing tools in RSM software [1,2]. Toxicity assessment of amines is a top priority for analyzing their negative environmental impact, and the toxicity of each chemical is classified into four basic categories [2,72-75].

In this present work, a novel aqueous HMDA+DMAE amine blend was formed to evaluate its performance by considering practical studies on CO_2 absorption and desorption. Equilibrium CO_2 loading and CO_2 absorption rate were the prime considerations under the CO_2 absorption study, and it was evaluated for the experiments at temperature (T) = 298.15–333.15 K, CO_2 partial pressure (P_{CO2}) = 10.13–25.33 kPa, mole fraction of HMDA (m_{HMDA}) = 0.05–0.20, and solution concentration (C) = 1–3 mol/L. Similarly, CO_2 desorption experiments were conducted at constant T = 393.15 K and P_{CO2} = 25.33 kPa. The cyclic equilibrium CO_2 loading, CO_2 desorption rate, cyclic capacity, heat duty, and

regeneration efficiency were calculated in CO_2 desorption experiments. pH and density measurements were done to evaluate the pH value of all CO_2-unloaded, CO_2-loaded, and CO_2-regenerated amine blends. ^{13}C NMR and FTIR analysis were used to characterize amine blend samples. Heat of CO_2 absorption (ΔH_{abs}), RSM-CCD modeling and optimization, and toxicity assessment were finally done.

4.2 Experimental section

4.2.1 Chemicals and equipment

HMDA (purity ≥ 98 %) and DMAE (purity ≥ 98 %) amines were purchased from Sigma-Alrich, U.S.A., and Sisco Research Laboratories (SRL) Private Limited, India, respectively. A novel aqueous HMDA+DMAE amine blend of various blend concentrations was prepared to capture CO_2 at different working conditions. MEA (purity ≥ 98 %) was acquired from Sd Fine Chemical Limited, India, and it was regarded as a standard to validate the CO_2 absorption setup and to compare the experimental values. Thermo Fisher Scientific (TFS) India Private Limited, India, has provided hydrochloric acid (HCl, purity = 35–37 %). 1 molar HCl stock solution was used for titrating the CO_2-loaded and CO_2-regenerated different aqueous amine blend solutions. To prepare a simulated flue gas mixture at lab scale, CO_2 and nitrogen (N_2) gas cylinders of 99.99 % purity were supplied from Linde India Limited, India. Dimethyl sulfoxide-d_6 (DMSO-d_6, purity ≥ 99 %) was acquired from Merk, Germany, for performing an NMR investigation of aqueous amine blend samples. High-purity double distilled water was produced on the laboratory scale. All the amine blend preparation and other tasks related to experimental work were carried out solely with this double distilled water. A list of chemicals with their specifications is shown in Table B5 of Appendix – B. Mass flow controllers that are

digitally controlled and have the following specifications: Model No: – MC-500SCCM-D-DB9M, ± 0.32 % reading or ± 0.02 % full scale was purchased from Alicat Scientific, India. United Phosphorus Limited, India, has provided a portable infrared CO_2 gas analyzer with the following specifications: Serial no. A-191 (PM), Gasboard–3800P, software version–1606.25, CO_2 analysis range: 0–100 % V/V. Toshniwal Instruments Mfg. Pvt. Ltd., Ajmer, India, supplied a digital pH meter with the following specifications: Model: 160 CL-54+, Serial No: 20K1595.

4.2.2 Experimental description of CO_2 absorption setup

Three key sections can easily summarize the whole description of the CO_2 absorption experimental setup: (a) Simulated flue gas mixture preparation; (b) Absorption of CO_2 gas in the novel aqueous HMDA+DMAE blend; (c) Monitoring of flue gas stream leaving off the amine blend. The schematic representation and complete description of the CO_2 absorption experimental setup are already shown in Figure 3.1 and section 3.2.3 of Chapter 3, respectively.

4.2.3 CO_2 absorption experiments

Temperature (T), CO_2 partial pressure (P_{CO2}), mole fraction of HMDA (m_{HMDA}), solution concentration (C), and absorption time (θ) were the five important independent variables on which the CO_2 absorption in the novel HMDA+DMAE amine blend depends. Experimental operating conditions: T = 298.15–333.15 K, P_{CO2} = 10.13–25.33 kPa, m_{HMDA} = 0.05–0.20, C = 1–3 mol/L, and θ = 10 hours (fully saturation state). As represented in Table B6 of Appendix – B, a manual run sheet for conducting experiments corresponding to all the aforementioned operating conditions was prepared. The information related to different CO_2 absorption experiments has already been incorporated

in Section 3.2.4 of Chapter 3. The equilibrium CO_2 loading (α) is calculated through the correlation as reported in our earlier study [1,2]:

$$\alpha = 12.1942 \times \frac{V_{CO_2}}{C_{blend} \times V_{CO_2\ saturated}} \times \frac{1}{(273.15+T)} \text{; mol } CO_2\text{/mol amine} \quad (4.1)$$

$$\text{Absorption capacity} = \alpha . C_{blend} \text{; mol } CO_2\text{/L solution} \quad (4.2)$$

Where α represents equilibrium CO_2 loading and V_{CO_2}, C_{blend}, $V_{CO_2\ saturated}$, T are the volume of CO_2 gas released (L) from the amine solution, amine blend concentration (mol/L), volume of CO_2 saturated amine sample (L), and room temperature (℃), respectively.

4.2.4 Experimental setup validation

It is crucial to prove the reliability of the experimental setup before conducting the actual CO_2 absorption experiments. The experimental results were validated through benchmark 30 wt% (or 5 mol/L) MEA by comparing the experimentally determined equilibrium CO_2 loading value with the previously published data [17,104-108]. The validation experiments were performed for different P_{CO_2}, ranging from 2.2 kPa to 31.6 kPa at a constant T = 313.15 K. The α value was determined to be 0.486, 0.525, 0.511, 0.589, 0.569, and 0.575 mol CO_2/mol amine corresponding to P_{CO_2} = 2.2, 7.0, 11.81, 15.0, 19.12, and 31.60 kPa, respectively. Table 4.1 shows the correlation between the experimental and literature data for α value at the aforementioned working conditions corresponding to 30 wt% MEA. The percentage average absolute relative deviation (% AARD) between the actual experimental runs and the data acquired from the literature was found to be 3.17 %, which is under 10 %. Therefore, based on these results, an experimental setup was authenticated and ready to be in operation for the estimation of α value during the CO_2 absorption study by using the novel aqueous HMDA+DMAE amine blend.

Table 4.1 Validation of the experimental setup by comparing the values of equilibrium CO_2 loading as determined by performing the actual experiments with the data obtained from the literature for 30 wt% MEA under particular operating conditions of temperature and CO_2 partial pressure[a].

S. No.	T (K)	P_{CO2} (kPa)	α_{exp} (mol CO_2/mol amine)	α_{lit} (mol CO_2/mol amine)	ARD (%)	Reference
1.	313.15	2.2	0.486	0.471	3.09	Shen and Li [104]
2.	313.15	7.0	0.525	0.510	2.85	Ji et al. [17]
3.	313.15	11.81	0.511	0.524	2.54	Aronu et al. [105]
4.	313.15	15.0	0.589	0.564	4.24	Gao et al. [106]
5.	313.15	19.12	0.569	0.585	2.81	Tong et al. [107]
6.	313.15	31.6	0.575	0.595	3.48	Lee et al. [108]
				AARD % =	3.17	

[a]Standard uncertainties of u are u(T) = 1 K, u(P_{CO2}) = 0.05 kPa, u(m_{HMDA}) = 0.001, u(C) = 0.01 mol/L and u(α) = 0.02 mol CO_2/mol amine.

4.2.5 CO_2 desorption setup description

It is necessary to conduct a desorption investigation on an amine blend to evaluate its performance. The CO_2-loaded HMDA+DMAE amine blend at complete CO_2 saturation was taken out from the bubble column reactor to perform the desorption study. The complete diagrammatic representation and entire description of the desorption setup are shown in Figure 3.2 and Section 3.2.5 of Chapter 3. The cyclic equilibrium CO_2 loading ($\Delta\alpha$) and cyclic capacity are two essential aspects of the desorption study, which are shown by Eq. (4.3) and Eq. (4.4), respectively.

$$\Delta\alpha = \alpha_{313.15\ \mathrm{K},\ 25.33\ \mathrm{kPa}} - \alpha_{393.15\ \mathrm{K},\ 25.33\ \mathrm{kPa}}\ ;\ \text{mol } CO_2\text{/mol amine} \quad (4.3)$$

$$\text{Cyclic capacity} = \Delta\alpha.\, C_{\mathrm{blend}}\ ;\ \text{mol } CO_2\text{/L solution} \quad (4.4)$$

4.2.6 pH measurement

Amines are known to be basic in nature, but the pH value must be measured to determine the basicity value of any amine blend. A digitally operated pH meter (Model No.: 160 CL-54+; Serial No: 20K1595; and accuracy: $\pm$ 0.01) was purchased from Toshniwal Instruments Mfg. Pvt. Ltd., Ajmer, India. Standard buffer solutions with a value of 4, 7, and 9.18 were used to calibrate the pH meter before using it. The calibrated pH meter evaluated the basicity of CO_2-unloaded, CO_2-loaded, and CO_2-regenerated amine blend samples during the entire experiment. The CO_2 loading in the HMDA+DMAE amine blend sample showed a significant impact on pH value. Therefore, pH estimation was essential to verify the volume of CO_2 loaded in the novel amine blend.

4.2.7 Density measurement

Determining thermophysical parameters such as density is essential in designing a CO_2 absorption bubble column reactor, as well as in process modeling, simulation, and

optimization of the CO_2 capture process [79-82]. The density of the CO_2-unloaded, CO_2-loaded, and CO_2-regenerated novel HMDA+DMAE amine blend samples was measured through portable density meter DMA^{TM} 35 (Serial number: 82907440; Weight: 660 g; Dimensions (L × W × H): 245 mm × 103 mm × 126 mm; Accuracy: 0.001 g/cm^3; Reproducibility: 0.0007 g/cm^3; Measuring range: 0 g/cm^3 to 3 g/cm^3), which was procured by Anton Paar India Private Limited, Haryana, India. Deionized water aided in calibrating the density meter, ensuring the precision of the measurement. Before measuring the density of any sample, the density meter's U-tube was thoroughly cleaned with acetone. All the experiments were conducted at atmospheric pressure. The sample density was assessed three times, and the average value was chosen.

4.2.8 ^{13}C NMR characterization

NMR spectroscopy is a robust, non-invasive analytical method used to analyze qualitative and quantitative results corresponding to the CO_2-unloaded, CO_2-loaded, and CO_2-regenerated amine blends [22,29,67,83]. NMR study focuses on atoms that exhibit magnetic moment in which the atom's spin quantum number is greater than zero [84]. The distribution of chemical species can be evaluated by NMR technique to validate the reaction mechanism. When doing NMR spectroscopy, there are essentially three isotopic approaches available to determine the relative peaks of any chemical species, which are ^{1}H, ^{13}C, and ^{15}N [67]. To study the behavior of the amine-CO_2-H_2O system, ^{1}H and ^{13}C are the most common techniques that most researchers have adopted. Characterization and quantification of any unknown compound can be done without using any standard reference, which is the most significant achievement of NMR spectroscopy. The reaction mechanism of a novel aqueous HMDA+DMAE blend has been discussed in section 4.3.

^{13}C NMR spectroscopy provides information about the intermediate species, i.e., H_2NCOO^-, HCO_3^-, CO_3^{2-}, $HMDAH^+$ and $DMAEH^+$ formed during the entire reaction.

The NMR experiments were performed with the OneBay NMR spectrometer instrument. The instrument was designed by the company: BRUKER BioSpin INTERNATIONAL AG; Model specification: AVH D 500 AVANCE III HD 500 MHz. Inside the NMR tubes, 0.6 ml solutions of CO_2-unloaded, CO_2-loaded, and CO_2-regenerated samples were placed, and all of these samples were characterized by the ^{13}C NMR spectroscopy at 298.15 K temperature [1-4,64-66]. DMSO-d_6 has been regarded as a deuterium lock that provides the proper signaling; therefore, 0.3 ml of DMSO-d_6 was introduced in every amine sample [85]. For internal referencing, the compound Tetramethylsilane ($(CH_3)_4Si$) with a chemical shift of 0.00 ppm was used during the investigation. The operating parameters were as follows:

- Operating spectral frequency = 125.8131145 MHz
- Time delay = 2 s
- Spectral width = 29761.904 Hz
- Total no. of scans = 256
- Acquisition time = 1.101 s

4.2.9 FTIR characterization

FTIR spectroscopy is an analytical characterization method that helps in determining the chemical bonds along with the functional groups present in any organic sample [17,86,87]. Samples with the physical state of liquid, powder form, solutions, pastes, and fibers can be characterized with this technique [87]. FTIR investigation of functional group and chemical bonding associated with CO_2-unloaded, CO_2-loaded, and CO_2-regenerated amine blend

solutions was done through the FTIR spectrophotometer instrument (Model: Nicolet iS5; Company: THERMO Electron Scientific Instruments LLC, USA). The KBr pellet sampling approach was used to record infrared spectra in the 4000–400 cm^{-1} region. The resolutions and number of scans chosen for the FTIR study were 4 cm^{-1} and 32, respectively. Correlation between transmittance (%) and the wavenumber (cm^{-1}) was used to analyze the chemical bonds and functional groups present in different amine blend samples.

4.2.10 Heat duty and regeneration efficiency

It was vital to evaluate the values of heat duty and regeneration efficiency to judge the performance of the novel aqueous HMDA+DMAE amine blend for post-combustion CO_2 capture. According to Figure 3.2 of Chapter 3, a hot plate heated the novel amine blend solution externally and served as a heating medium. Therefore, heat duty is defined as the ratio of steady-state heat transfer from the silicon oil to the regeneration reactor to the amount of CO_2 released from the amine sample [2,44]. Correlation by Fourier yielded heat transfer value, which can be expressed as:

$$q = \frac{KAdT}{dx}\ ; J/s \tag{4.5}$$

Where q is the steady state heat transfer (J/s); K denotes the thermal conductivity of the Pyrex glass material ($\frac{W}{m.K}$); A represents the spherical surface area of the regeneration reactor normal to heat flow (m^2); dT signifies the temperature difference between the oil bath and the amine blend solution (K); dx is the thickness of the regeneration reactor (m^2).

The cyclic capacity of the novel amine blend is an essential parameter that was used to calculate the amount of CO_2 removed during the regeneration experiment, and it can be estimated as follows:

$$CO_2 \text{ removed} = \frac{\Delta\alpha \times C_{blend} \times V}{t} \text{ ; mol } CO_2/s \quad (4.6)$$

Where $\Delta\alpha . C_{blend}$ represents the cyclic capacity of the novel amine blend (mol CO_2/L solution); V is the volume of the amine sample; t denotes the desorption time (sec). On performing desorption experiments, it was discovered that around 30 min of the experiment, the amine blend sample showed nearly constant equilibrium CO_2 loading.

According to Eq. 4.5 and Eq. 4.6, the overall formula for evaluating heat duty can be expressed as:

$$Q_{Reg} = \frac{q}{CO_2 \text{ removed}} \text{ ; kJ/mol } CO_2 \quad (4.7)$$

Gautam and Mondal [2], Muchan et al. [24], and Narku-Tetteh et al. [44] also used a similar above-mentioned correlation for heat duty estimation in their investigations.

$$\text{Regeneration efficiency } (\%) = \left(\frac{\text{Cyclic capacity}}{\text{Absorption capacity}}\right) \times 100 \quad (4.8)$$

4.2.11 CO_2 absorption and desorption rate

In the industrial sector, the CO_2 absorption and desorption rate are essential for assessing the performance of amine and its various blends for post-combustion CO_2 capture. The amines showing a high rate of CO_2 absorption are always advantageous over other amines. The absorption rate directly impacts the absorption column size, and if the absorption rate is fast, it needs a smaller size of the absorption column and vice-versa [4,6]. As a result, the overall cost of the equipment is reduced. Therefore, absorption and desorption rates are critical aspects that affect the overall cost of the system. The absorption rate is determined by the linear slope of the plot between CO_2 loading and absorption time. Another way of understanding the CO_2 absorption rate is through conducting the experiments at similar operating conditions (only varying the molar ratio of the activator) and analyzing the

change in equilibrium CO_2 loading with respect to time for various aqueous amine blends and those amine blends with high equilibrium CO_2 loading at constant operating time exhibits high CO_2 absorption rate and vice-versa [6]. Similarly, the linear slope signifies the desorption rate when plotting the graph between the CO_2 loading vs. desorption time.

4.2.12 Heat of CO_2 absorption (ΔH_{abs})

When CO_2 gas molecules interact with amine blend solutions, CO_2 absorption takes place, and the solution releases heat, known as the heat of CO_2 absorption. The heat produced during this process increases the solution temperature and ultimately reduces the equilibrium CO_2 loading [34,47]. The basic theoretical information about the heat of CO_2 absorption has been incorporated in the B7 of Appendix – B. It is discovered that the ΔH_{abs} is a function of T & P_{CO2}, and for this present experimental work, T varied from 298.15 to 333.15 K whereas, P_{CO2} ranged from 10.13 to 25.33 kPa. ΔH_{abs} value can be determined easily after calculating the α value data for the novel HMDA+DMAE amine blend. Using the Gibbs-Helmholtz equation, the ΔH_{abs} value for any aqueous amine blend system may be computed as follows:

$$\frac{d[\ln(P_{CO2})]}{d(\frac{1}{T})} = \frac{\Delta H_{abs}}{R} \tag{4.9}$$

Where $P_{CO2,}$ T, ΔH_{abs}, and R denotes CO_2 partial pressure (kPa), working temperature (K), heat of CO_2 absorption (J/mol), and universal gas constant [J/(mol.K)], respectively. The multiplication of slope plotted in between $\ln(P_{CO2})$ vs. $(\frac{1}{T})$ by R provides the value of ΔH_{abs}. Several data sets of P_{CO2} and $(\frac{1}{T})$ were chosen for the estimation of the heat of CO_2 absorption for those solutions having approximately same α value. The physical

significance of the Gibbs-Helmholtz equation can be found in most of the previously published research articles [8,24,89-93].

4.2.13 Designing of experimental runs by RSM software

RSM is a powerful statistical tool that optimizes approximately all challenging engineering and non-engineering problems. RSM optimizes the final response corresponding to various sets of operating conditions. In this work, the CO_2 capturing was accomplished by the novel aqueous HMDA+DMAE amine blend. Therefore, α value as a final response was optimized by this software-based technique. Trial version 8.0.6 of the Design-Expert® software was employed to optimize all the experiments in a very systematic and easy manner. The complete system was comprised of four independent variables: Temperature (T), partial pressure of CO_2 (P_{CO2}), mole fraction of HMDA (m_{HMDA}), and solution concentration (C). Range of input values of independent variables (i.e., numeric factors): T = 298.15–333.15 K, P_{CO2} = 10.13–25.33 kPa, m_{HMDA} = 0.05–0.20, and C = 1–3 mol/L. The theoretical information associated with designing of experimental run sets from RSM has already been discussed in Section 3.2.9 of Chapter 3.

4.2.14 Toxicity analysis

It is crucial to find out the toxicity of the amine blend solution before adopting it for any industrial application [94]. Since amines have the potential to chemically react with different components of the flue gas, i.e., O_2, CO_2, CH_4, N_2O, SO_X, NO_X, etc., to produce degradable products, few of those products lead to hazardous impacts on the atmosphere. When exposed to the environment, amines undergo different chemical processes, including absorption, adsorption, degradation, and photolysis. Due to amine exposure in the environment, aldehydes, nitramines, amides, and nitrosamines products are formed [95].

Amongst these products, nitrosamine is considered a toxic degradable compound that is highly carcinogenic, pollutes water resources, and harms aquatic life. Information regarding the toxicity level of different amines is helpful in forecasting the dangerous effects of amines on the environment and human beings. Amines with high toxicity levels are not recommended for CO_2 capture purposes, and this should always be kept in mind when choosing an amine.

Acute toxicity focuses on the lethal effect of any chemical that can be categorized into three types: oral, dermal, and inhalation exposure [96]. Toxicity causes in living beings due to the ingestion of chemicals is called oral toxicity, toxicity due to the absorption of chemicals on the skin is known as dermal toxicity and toxicity due to chemical inhalation is called inhalation toxicity. For this present work, oral toxicity of amines was targeted, which may be easily comprehended through the help of lethal dose (LD_{50} value) information obtained from the material safety data sheet (MSDS) of specific amines. LD_{50} is the chemical dose that causes mortality amongst the 50 % population of the animals chosen for the study that is available in a group, and its unit is mg/Kg [77,96,97]. Therefore, it can be noted that if the value of LD_{50} is higher, then the amine toxicity is low and vice-versa [98]. Environmental Protection Agency (EPA), based on LD_{50} values, has classified the toxicity of different chemicals into 4 important categories. Amine classification based on toxicity and LD_{50} value has been reported in the B8 of Appendix – B.

4.3 Chemical reactions of the novel amine blend system (HMDA + DMAE + H_2O + CO_2)

There are mainly three mechanisms, namely the Zwitterion mechanism, Termolecular mechanism, and Base-catalyzed hydration mechanism, which exist to define the amine

reaction behavior with CO_2 [3,23,39,64]. Most researchers have relied on and targeted the zwitterion mechanism to discuss the chemically reacting alkanolamine solvents.

1. Zwitterion mechanism

The primary or secondary amines chemically react with the CO_2 gas molecules according to the zwitterion mechanism. Caplow [99] was the first to suggest this reaction mechanism, and further investigations have been done by Danckwerts [100]. This zwitterion mechanism finds its applications in aqueous alkanolamine solutions. According to this mechanism, when the primary or secondary amine's first molecule reacts with CO_2 gas molecules, a chemical reaction occurs between them, forming a zwitterion [19,45]. Further, this zwitterion undergoes deprotonation, and carbamate is formed while reacting with a second amine molecule that acts as a base. Carbamate, bicarbonate, and carbonate are major products formed during the reaction of primary or secondary amines with the CO_2 molecule [39].

Zwitterion formation step: $CO_2 + R_1R_2NH \leftrightarrow R_1R_2NH^+COO^-$ (4.10)

Zwitterion deprotonation step: $R_1R_2NH^+COO^- + B \leftrightarrow R_1R_2NCOO^- + BH^+$ (4.11)

Where R_1R_2NH is the secondary amine, $R_1R_2NH^+COO^-$ is the zwitterion, and B is the base.

2. Termolecular mechanism

Crooks and Donnellan [101] were the first to devise and develop this mechanism. It was claimed that when CO_2 gas molecules react with the amine, the formation of zwitterion occurs, and further deprotonation steps occur simultaneously. Da Silva and Svendsen [102] later reviewed this mechanism by initially adopting a similar concept given by Danckwerts.

Reaction step: $CO_2 + R_1R_2NH + B \leftrightarrow R_1R_2NCOO^- + BH^+$ (4.12)

3. Base-catalyzed hydration mechanism: The mechanism is applicable when tertiary alkanolamine-based solvents are employed to capture CO_2. Tertiary amines cannot react directly with CO_2 but act as a base catalyst for CO_2 hydration. This mechanism was developed by Donaldson and Nguyen [103] in 1980.

Reaction step: $CO_2 + R_1R_2R_3N + H_2O \leftrightarrow R_1R_2R_3NH^+ + HCO_3^-$ (4.13)

Chemical reactions are mostly evaluated by the type of amine utilized in the CO_2 reaction. When HMDA is blended with DMAE in the aqueous solution, a novel amine blend forms, and various sets of chemical reactions occur when this blend physically reacts with CO_2. These chemical reactions involve CO_2 solubility in the aqueous phase, H_2O dissociation, HCO_3^- and CO_3^{2-} formation, and HMDA and DMAE intermediate reactions. Using ^{13}C NMR and FTIR analyses, ionic species available in the novel HMDA+DMAE amine blend system in CO_2-unloaded, CO_2-loaded, and CO_2-regenerated samples can be verified. The following are the complete sets of chemical reactions:

Physical CO_2 solubility:

$$CO_2\ (g) \overset{H_{CO_2}}{\longleftrightarrow} CO_2\ (aq.) \quad (4.14)$$

Dissociation of H_2O molecule [32**]:**

$$H_2O \overset{K1}{\leftrightarrow} H^+ + OH^- \quad (4.15)$$

Bicarbonate formation [38,48**]:**

$$CO_2 + H_2O \overset{K2}{\leftrightarrow} HCO_3^- + H^+ \quad (4.16)$$

$$CO_2 + OH^- \overset{K3}{\leftrightarrow} HCO_3^- \quad (4.17)$$

Carbonate formation [64**]:**

$$HCO_3^- \overset{K4}{\leftrightarrow} CO_3^{2-} + H^+ \quad (4.18)$$

HMDA intermediate reactions [37,47**]:**

$$HMDA + CO_2 \overset{K5}{\leftrightarrow} HMDA^+COO^- \quad (4.19)$$

$$HMDA + HMDA^+COO^- \overset{K6}{\leftrightarrow} HMDA^+ + HMDACOO^- \text{ (Monocarbamate formation)} \quad (4.20)$$

$$HMDAH^+ + H_2O \overset{K7}{\leftrightarrow} HMDA + H_3O^+ \text{ (Amine deprotonation)} \quad (4.21)$$

$$HMDACOO^- + CO_2 + H_2O \overset{K8}{\leftrightarrow} H_3O^+ + HMDA(COO^-)_2 \text{ (Bicarbamate formation)} \quad (4.22)$$

$$HMDACOO^- + H_2O \overset{K9}{\leftrightarrow} HCO_3^- + HMDA \text{ (Bicarbonate formation)} \quad (4.23)$$

$$HMDA + CO_2 + H_2O \overset{K10}{\longleftrightarrow} HCO_3^- + HMDAH^+ \quad (4.24)$$

DMAE intermediate reactions [1,2,45,57,58**]:**

$$DMAE + H^+ \overset{K11}{\longleftrightarrow} DMAEH^+ \text{ (Protonation of DMAE)} \quad (4.25)$$

$$DMAE + CO_2 + H_2O \overset{K12}{\longleftrightarrow} DMAEH^+ + HCO_3^- \quad (4.26)$$

Overall chemical reaction of the system:

$$2HMDA + 3DMAE + 4CO_2 + 4H_2O \overset{K13}{\longleftrightarrow} 3HCO_3^- + CO_3^{2-} + 2HMDAH^+ + 3DMAEH^+ \quad (4.27)$$

H_{CO_2} is the Henry's constant, Eq. 4.14 to Eq. 4.27 is the chemical reactions of HMDA+DMAE aqueous amine blend system, K1 to K13 is chemical reaction equilibrium.

4.4 Results and discussion

4.4.1 Equilibrium CO_2 loading for the novel HMDA+DMAE amine blend

α value was calculated by conducting CO_2 absorption experiments at the definite operating condition by a novel aqueous HMDA+DMAE amine blend. α value is an essential factor that provides an idea about the performance of any amine blend, which is an important aspect in considering its implementation in the real industrial process. Any amine

solvent with high α value is regarded as highly suitable and efficient in CO_2 capture from flue gas. Gas mixing chamber, bubble column reactor, water bath, condenser, silica gel bed, CO_2 gas analyzer, etc. were some of the important auxiliaries that aided in the estimation of α value. Operating conditions are as follows: temperature (T) = 298.15–333.15 K, CO_2 partial pressure (P_{CO2}) = 10.13–25.33 kPa, mole fraction of HMDA (m_{HMDA}) = 0.05–0.20, and solution concentration (C) = 1–3 mol/L. A manual run sheet with 40 experiments was created according to the operating conditions, and the effect of these operational parameters on α value was correlated. Similarly, Design-Expert® software trial version 8.0.6 has created 30 experimental run sets by adopting CCD, of which 6 were due to the central point and 24 were due to non-central points. Therefore, a total of 70 experiments were conducted in the laboratory at 1 atmospheric pressure. The relationship among the α value and different operating conditions generated by manual run sets is tabulated in Table B6 of Appendix – B with a % AARD of 3.06, which is highly acceptable.

4.4.1.1 Effect of temperature on equilibrium CO_2 loading for novel aqueous HMDA+DMAE amine blend

This section discusses about how the variation of temperature affected the α value by using the novel aqueous HMDA+DMAE amine blend. To judge the effect of T on α value, the experiments were performed in the temperature (T) ranging from 298.15 to 333.15 K, whereas CO_2 partial pressure and mole fraction of HMDA remained constant, i.e., 25.33 kPa and 0.20, respectively. The effect of temperature was analyzed for the aforementioned operating conditions for different solution concentrations, i.e., C = 1, 2, and 3 mol/L. Figure 4.1 (a) represents the relationship between the T and α. It was discovered that α value was high at low temperature, and further, it started decreasing with increasing temperature.

Therefore, minimum and maximum equilibrium CO_2 loading for C = 1, 2, and 3 mol/L was attained at a T = 298.15 K and 333.15 K, respectively. The main reason for this scenario is stated by 'Le-Chatelier's principle'. This principle dictates that as the temperature rises, the gas-liquid equilibrium shifts in the backward direction; therefore, the solubility of a gas in the novel amine blend is highest at the lowest temperature and vice-versa [1,2,8,9,13,109]. Another important reason is that desorption dominates over absorption at high temperature because the CO_2 gas molecules try to escape from the novel amine blend, reducing equilibrium CO_2 loading [1,2,27]. Therefore, from the entire discussion till now, it can be concluded that high α value is obtained at low temperature and vice-versa.

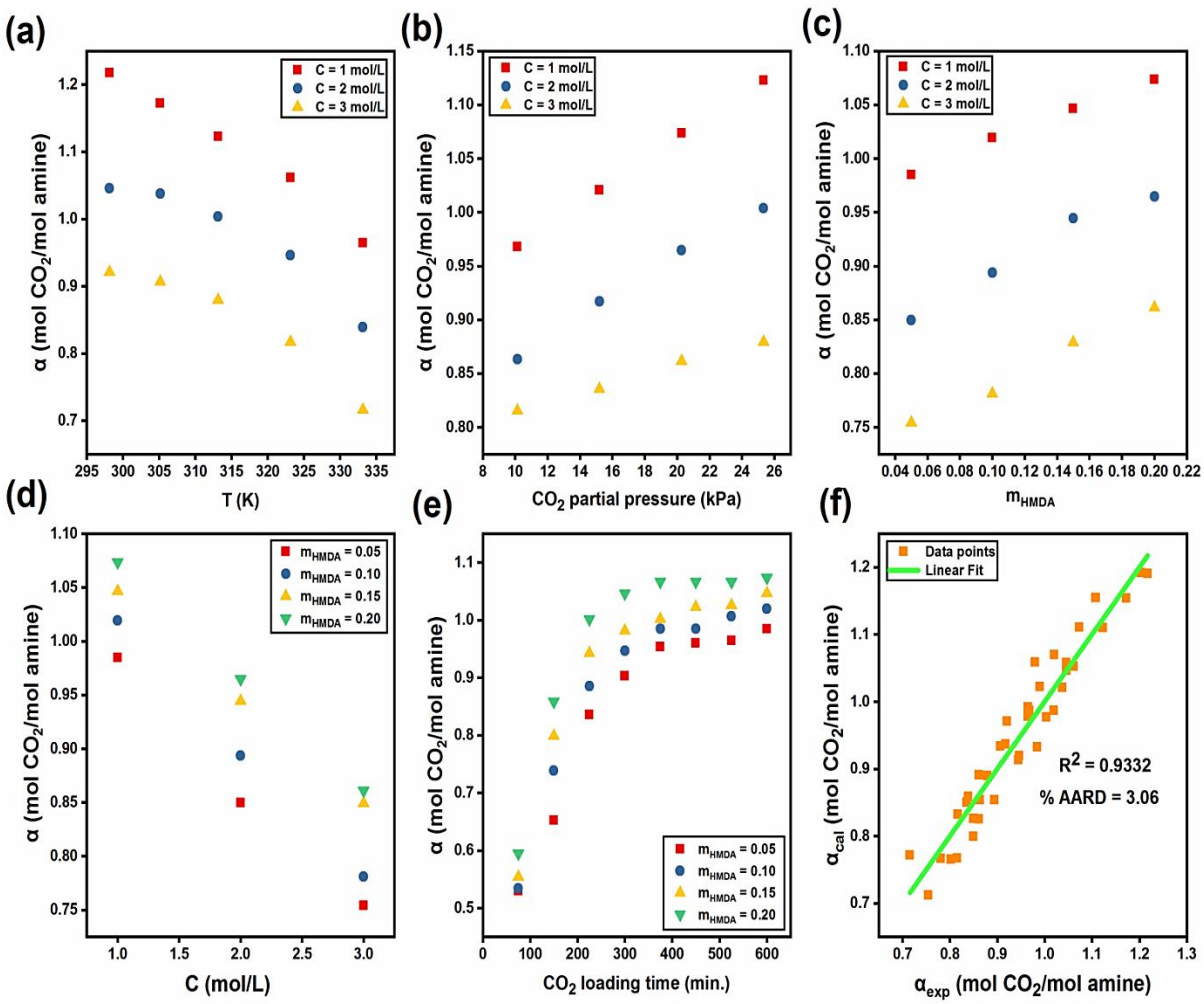

Figure 4.1 (a) Effect of temperature (T) on equilibrium CO_2 loading (α) for C = 1, 2, and 3 mol/L at constant P_{CO2} = 25.33 kPa and m_{HMDA} = 0.20; (b) Effect of CO_2 partial pressure (P_{CO2}) on equilibrium CO_2 loading (α) for C = 1, 2, and 3 mol/L at constant T = 313.15 K and m_{HMDA} = 0.20; (c) Effect of mole fraction of HMDA (m_{HMDA}) on equilibrium CO_2 loading (α) for C = 1, 2, and 3 mol/L at constant P_{CO2} = 20.27 kPa and T = 313.15 K; (d) Effect of solution concentration (C) on equilibrium CO_2 loading (α) for m_{HMDA} = 0.05, 0.10, 0.15, 0.20 at constant T = 313.15 K and P_{CO2} = 20.27 kPa; (e) Effect of CO_2 loading time on equilibrium CO_2 loading (α) for m_{HMDA} = 0.05, 0.10, 0.15, and 0.20 at constant C = 1 mol/L, T = 313.15 K, and P_{CO2} = 20.27 kPa; (f) Parity plot of experimental (α_{exp}) and calculated (α_{cal}) CO_2 loading for the novel aqueous amine blend of HMDA+DMAE.

4.4.1.2 Effect of CO_2 partial pressure on equilibrium CO_2 loading for novel aqueous HMDA+DMAE amine blend

To check the CO_2 partial pressure effect, the experiments were done at a constant T and m_{HMDA} of 313.15 K and 0.20, respectively. The variation of P_{CO2} was in the range of 10.13 to 25.33 kPa for different solution concentrations, i.e., C = 1, 2, and 3 mol/L. The purpose of selecting the above-mentioned pressure range is mainly to cover many chemical industries whose CO_2 gas composition during emission lies in the range of the present experimental condition of CO_2 partial pressure. The sources of CO_2 emissions through chemical industries include coal-fired power plants, cement industries, refineries, integrated steel mills, ethylene industries, blast furnaces, and so on. Figure 4.1 (b) represents the relationship between CO_2 partial pressure and equilibrium CO_2 loading. It was found that on raising the value of P_{CO2} the value of α also increased in the P_{CO2} range, i.e., from 10.13 to 25.33 kPa. The relationship between P_{CO2} and α was followed by all different solution concentrations, i.e., C = 1, 2, and 3 mol/L. Henry's law states that the solubility of any gas in a liquid is directly proportionate to its partial pressure. Therefore, on raising P_{CO2} value, the driving force increases, which also increases interfacial mass transfer, which leads to the dissolution of more CO_2 molecules available in the novel amine blend of HMDA+DMAE [9,19,27,76,109,110]. Based on α value data as presented in Table B6 of Appendix – B and Figure 4.1 (b), it is inferred that the novel aqueous amine blend perfectly obeys Henry's law. Evidence of following the linear relationship between P_{CO2} and α was also found in most of the previously published research articles [1,2,4,6,8,27]. When CO_2 gas reacts with an aqueous amine solution, it forms intermediate species, and these species

are carbamate, carbonate, and bicarbonate, which are authenticated by ^{13}C NMR and FTIR characterization techniques.

4.4.1.3 Effect of mole fraction of HMDA on equilibrium CO_2 loading for novel aqueous HMDA+DMAE amine blend

This section describes how raising the activator's mole fraction (i.e., HMDA) in a novel aqueous HMDA+DMAE amine blend affected α value. To judge the effect of m_{HMDA} on α, the experiments were done at a constant P_{CO2} and T, i.e., 20.27 kPa and 313.15 K, respectively. The m_{HMDA} was varied from 0.05 to 0.20, and its effect on α was observed for various solution concentrations, i.e., C = 1, 2, and 3 mol/L. Figure 4.1 (c) represents the relationship between the mole fraction of HMDA and equilibrium CO_2 loading. Most of the literature stated that primary and secondary amines, which are categorized as activators, can achieve the highest theoretical α value of 0.5 mol CO_2/mol amine [38,46]. Likewise, the tertiary amines are known as promoters, which are capable of achieving the maximum theoretical α value of 1 mol CO_2/mol amine [1,2,27]. As a result, blending the high kinetics HMDA with the low kinetics DMAE is always fruitful in achieving high equilibrium CO_2 loading, enhanced absorption rate, fabulous degradation resistance, reduced regeneration energy requirement, and so on. Therefore, the effect of the activator's mole fraction (HMDA) on the promoter (DMAE) has been analyzed in the above-mentioned operating conditions. It was noticed that on enhancing m_{HMDA} value from 0.05 to 0.20, α value also enhanced accordingly. The maximum and minimum α value was attained at P_{CO2} = 20.27 kPa and T = 313.15 K on varying m_{HMDA} from 0.05 to 0.20, for every C = 1, 2, and 3 mol/L. HMDA is a diamine with two primary amino groups present in its chemical structure, and the nitrogen atom in HMDA has a high partial atomic charge, leading to high

reactivity towards CO_2 compared with most conventional amines. Therefore, enhancing m_{HMDA} in the novel aqueous HMDA+DMAE amine blend also enhances the α value, which was also validated by the actual experimental runs [110]. Increasing the value of m_{HMDA} increases α, but at the same time, it also increases the ΔH_{abs} value, which is not fruitful. As a result, the range of m_{HMDA} was varied from 0.05 to 0.20, and further raising the m_{HMDA} will impart an enormous overall ΔH_{abs} value of the novel aqueous HMDA+DMAE amine blend, which is never recommended. Therefore, the selection of the mole fraction of the HMDA range was entirely based on the previously published articles **[**1,2,111,112**]**.

4.4.1.4 Effect of solution concentration on equilibrium CO_2 loading for novel aqueous HMDA+DMAE amine blend

This section deals with how increasing the solution concentration affected the α value of a novel aqueous HMDA+DMAE amine blend. It is always essential to choose the appropriate solution concentration to attain the maximum α value. To examine the effect of solution concentration, the experiments were done at constant T and P_{CO2}, i.e., 313.15 K and 20.27 kPa, respectively. Solution concentration novel amine blend was changed from 1 to 3 mol/L, and its effect on α value was determined for various mole fractions of HMDA, i.e., m_{HMDA} = 0.05, 0.10, 0.15, and 0.20. Figure 4.1 (d) signifies the established correlation between the solution concentration and equilibrium CO_2 loading. It was discovered that when C varied from 1 to 3 mol/L for every definite m_{HMDA} value, the α value decreased accordingly. Based on the above statement, the general trend of α value with respect to C is as follows: 1 mol/L > 2 mol/L > 3 mol/L [2,110]. The prime reason is that, on increasing the solution concentration, the steric hindrance of the solution increases, which acts as a

barrier for converting carbamate into bicarbonate in the gas-liquid reaction, which finally decreases the equilibrium CO_2 loading [1,2,9,27,109,112]. Another major reason is based on Le-Chatelier's principle; according to it, as the solution concentration of the amine increases, the reacting amine molecules also enhances; however, simultaneously, the amine to CO_2 ratio also rises, resulting in the decrease of α value [2,8]. Finally, this section concludes that the maximum α value can be attained at the lower value of concentration and vice-versa. Therefore, the experimental investigation (Table B6 of Appendix – B; Run 09) for the novel HMDA+DMAE amine blend determined $\alpha_{maximum}$ = 1.2174 mol CO_2/mol amine, which was attained at T = 298.15 K, P_{CO2} = 25.33 kPa, m_{HMDA} = 0.20, and C = 1 mol/L.

4.4.1.5 Effect of time on equilibrium CO_2 loading for novel aqueous HMDA+DMAE amine blend

Absorption time is an important aspect that signifies the duration of the CO_2 absorption within the amine blend. It provides information about the reaction time for any specific amine blend, during which the aqueous amine blend solution became CO_2-loaded. Various amine blends have different equilibrium absorption times to attain the situation of CO_2 loading at equilibrium conditions. At the start of the experiments, the rate of CO_2 absorption is fast, and after sometimes, it reduces as time proceeds [6,19,30,78]. The main reason for this scenario is that in the beginning, the amine blend solution tends to absorb more CO_2 gas [2]. When the amine blend solution is about to be CO_2-saturated, then further addition of CO_2 in the solution does not impart much effect on CO_2 loading, and this scenario arises at maximum operating time. To examine the effect of absorption time on α value for the novel aqueous HMDA+DMAE amine blend, the experiments were done at

constant T and P_{CO2}, i.e., 313.15 K and 20.27 kPa, respectively. C = 1 mol/L was selected to examine the absorption time effect for different mole fractions of HMDA, i.e., m_{HMDA} = 0.05, 0.10, 0.15, and 0.20. Figure 4.1 (e) shows the influence of CO_2 loading time on equilibrium CO_2 loading.

All experiments of this novel blend were conducted for 10 hours of absorption time. It was discovered from experimental results that up to 300 min of absorption time, the CO_2 absorption rate was very fast, and enhanced CO_2 loading in the amine blend was seen. Up to 300 min, this increment was approximately linear, but after this absorption time, such increment of CO_2 loading was drastically diminished. After 500 min, a negligible increase in CO_2 loading was seen; therefore, it clearly indicated that the novel aqueous HMDA+DMAE amine blend was entirely CO_2-saturated, and the novel solution attained the scenario of equilibrium CO_2 loading.

4.4.2 An empirical model development for the novel aqueous amine blend of HMDA+DMAE

Initially, experiments based on various operating conditions were done on the laboratory scale, but it was most important to validate the experimental results. As a result, creating an empirical model for validating the experimental values was critical in proving the experiments' veracity. An empirical modeling equation was created for correlating α value with all the independent variables as a final response. These independent variables are T (K), P_{CO2} (kPa), m_{HMDA}, and C (mol/L). Validity of the empirical modeling equation: T = 298.15–333.15 K, P_{CO2} = 10.13–25.33 kPa, m_{HMDA} = 0.05–0.20, and C = 1–3 mol/L. The developed model can be used to calculate α value for the novel HMDA+DMAE amine

blend. The empirical modeling equation can be represented using the parameters stated above as follows:

$$\alpha_{cal} = a_1 + a_2T + a_3T^2 + a_4P_{CO2} + a_5P_{CO2}^2 + a_6m_{HMDA} + a_7m_{HMDA}^2 + a_8C + a_9C^2 \quad (4.28)$$

In this modeling equation, α_{cal} is the equilibrium CO_2 loading (mol CO_2/mol amine) calculated by the model; a_1 to a_9 be the unknown coefficients and the rest of the expressions of Eq. 4.28 have previously been discussed.

This established modeling equation's significance is extremely reliable because it has been found in most of the previously published literature [1,2,27,111,112]. Excel software approach corresponding to various experimental data sets was helpful in determining unknown coefficients. All such values of unknown coefficients associated with the aforementioned equation have been listed in Table 4.2.

Table 4.2 Values of the unknown coefficients involved in the empirical modeling associated with the experimental data sets.

Coefficient	Value	Coefficient	Value	Coefficient	Value
a_1	1.001585347	a_4	0.037120743	a_7	0.984553532
a_2	0.003341859	a_5	– 0.00081907	a_8	– 0.20176533
a_3	– 0.000014301	a_6	0.945415503	a_9	0.022901672

On the basis of these unknown coefficient values, the calculated value of equilibrium CO_2 loading (α_{cal}) can be estimated by this developed modeling equation. Now, the values of α_{exp} and α_{cal} were available, so their deviation was calculated. The percentage absolute relative deviation (% ARD) and % AARD were estimated as:

$$\% \text{ ARD} = \frac{|\alpha_{exp} - \alpha_{cal}|}{\alpha_{exp}} \quad (4.29)$$

$$\% \text{ AARD} = \frac{1}{N} \times \sum_{i=1}^{N} \frac{|\alpha_{exp} - \alpha_{cal}|}{\alpha_{exp}} \quad (4.30)$$

Where N is the number of experimental data sets, α_{exp} is the actual value of equilibrium CO_2 loading obtained after performing the laboratory experiments (Eq. 4.1), α_{cal} is the calculated value of equilibrium CO_2 loading by the developed model equation (Eq. 4.28). While considering the whole experimental data sets of Table B6 of Appendix – B, the % AARD was found to be 3.06 %, which is a fantastic linear correlation between α_{exp} and α_{cal}, and the same is shown in Figure 4.1 (f). Therefore, the developed modeling equation was highly reliable, accurate, acceptable, and ultimately it provided the best possible results.

4.4.3 Investigation of CO_2 desorption results

It has already been discussed that the CO_2-loaded HMDA+DMAE amine solution was acquired from the CO_2 absorbing bubble column to perform desorption experiments to judge the performance of the novel HMDA+DMAE amine blend. In the industrial world, cyclic equilibrium CO_2 loading and cyclic capacities are two critical parameters that must be focused on for the selection of any amine blend that is used to capture CO_2 [1,2,8,88,98,113]. The cyclic equilibrium CO_2 loading ($\Delta\alpha$) is defined as the difference between α values at a particular temperature and the temperature at which the amine regeneration is performed and P_{CO2} remains constant throughout the process [12]. $\Delta\alpha$ value for this novel blend was estimated at two different temperatures, i.e., T = 313.15 and 393.15 K at a constant P_{CO2} = 25.33 kPa. Likewise, the ability of amine to capture CO_2 per

mole amine per amine cycle through the CO_2 capture unit is defined as the cyclic capacity [2,19,44].

Initially, CO_2-loaded samples with different solution concentrations, i.e., C = 1, 2, and 3 mol/L, at constant m_{HMDA} = 0.20 and P_{CO2} = 25.33 kPa, were targeted to investigate $\Delta\alpha$ and cyclic capacity of the novel blend. According to these operating conditions, run no. 7, 21, and 34 were selected, and these operating conditions have been shown in Table B6 of Appendix – B. In this chain, 30 wt% MEA solution was regenerated and used to evaluate the above-mentioned process parameters to compare the experimental results. When the desorption experiments were performed, the CO_2-regenerated samples were taken off from the desorption reactor and titrated thrice, and their average value was finally considered for further investigation. At T = 313.15 K and P_{CO2} = 25.33 kPa, 30 wt% MEA solution has yielded α = 0.6313 mol CO_2/mol amine, $\Delta\alpha$ = 0.1972 mol CO_2/mol amine and cyclic capacity = 0.986 mol CO_2/L solution. These results were also authenticated by the previous investigation done by Pandey and Mondal [8]. After 30 min of desorption, the amine blend solutions lead to final CO_2 loading of 0.5366, 0.3662, and 0.3544 mol CO_2/mol amine, corresponding to run no. 7 (C = 1 mol/L), 21 (C = 2 mol/L), and 34 (C = 3 mol/L). The cyclic equilibrium CO_2 loading and cyclic capacity of the novel aqueous amine blend of HMDA+DMAE are shown in Figure 4.2. It was found that the $\Delta\alpha$ value of solutions with concentration, i.e., C = 1 (run no. 7), 2 (run 21), and 3 mol/L (run 34), were 0.5862, 0.6375, and 0.5317 mol CO_2/mol amine. It was found that the cyclic capacity of 3 mol/L solution was 1.5951 mol CO_2/L solution, which is 61.77 % greater than 30 wt% benchmark MEA. This is because the general trends of CO_2 cyclic capacity based on amine classification can be expressed as: Diamines > 3° amines > 2° amines > 1° amines [3]**.** Therefore, HMDA is a

diamine, and DMAE is 3° amines, as already discussed in the introduction section, so the novel aqueous HMDA+DMAE blend resulted in a high value of cyclic capacity. This commendable result of cyclic capacity for the novel aqueous HMDA+DMAE blend will require a small size of the CO_2 capture unit that will need a lower circulation rate of solvent and ultimately result in a reduction in the entire capital cost [1,13,88].

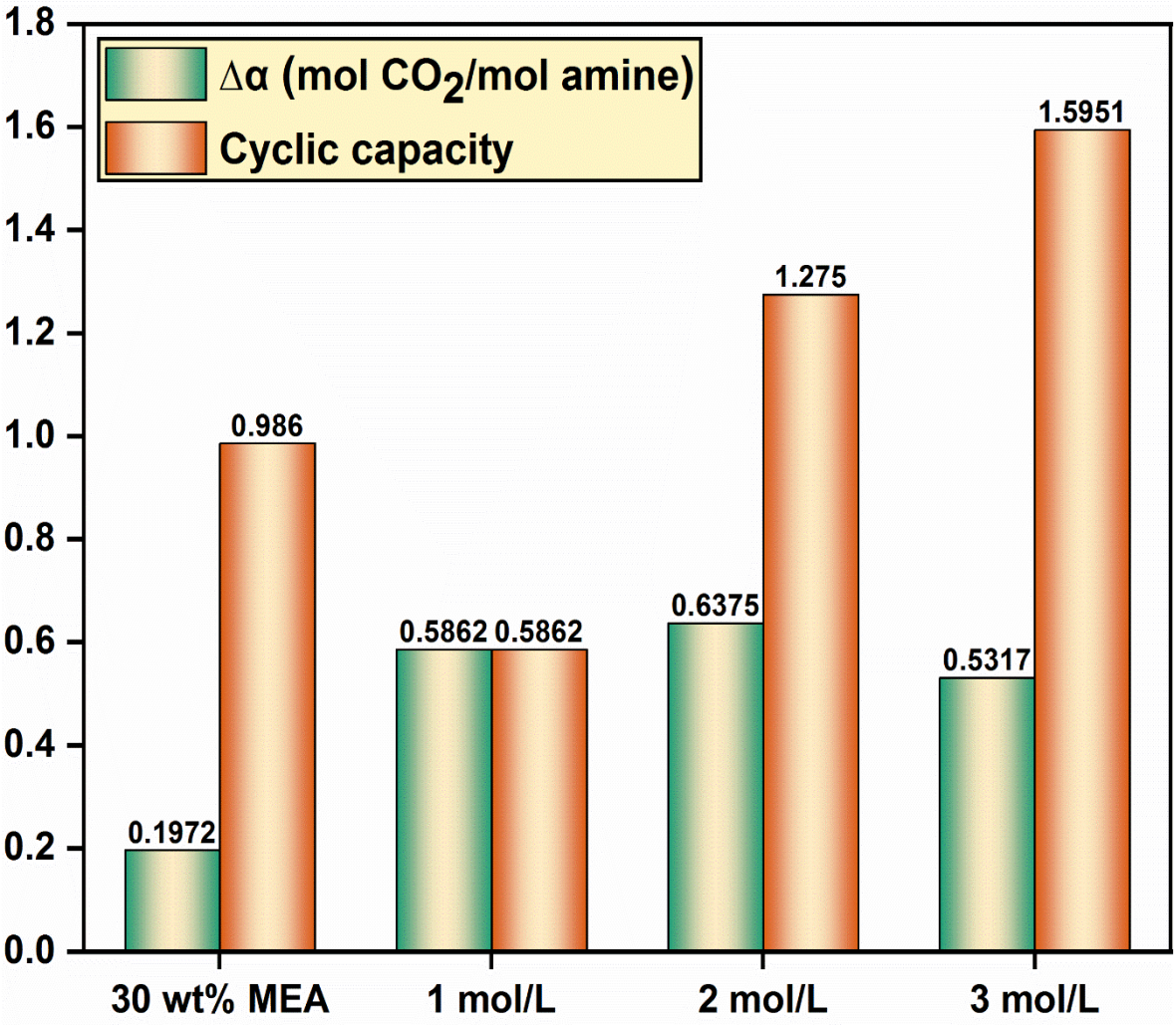

Figure 4.2 Cyclic equilibrium CO_2 loading (Δα) and cyclic capacity for 30 wt% MEA and for solution concentrations, i.e., C = 1, 2, and 3 mol/L at T = 313.15 K, P_{CO2} = 25.33 kPa, and m_{HMDA}= 0.20 for the novel aqueous amine blend of HMDA+DMAE for post-combustion CO_2 capture.

4.4.4 Effect of CO_2 loading on pH

The nature of the amines is basic, and their basicity depends upon the concentration of the aqueous solutions, and it is universally known that the CO_2 gas is acidic in nature [2,11,12,14]. Regarding CO_2 capture behavior, pH is a critical factor to consider while judging the performance of any amine blend solvent [12]. Therefore, a considerable variation in the solution pH was observed when a novel aqueous HMDA+DMAE blend interacted with the CO_2. This change in pH value provides information about the level of CO_2 loading in the amine blend. Experimental results showed that CO_2 loading is inversely proportional to the solution pH [11]. The entire family of amines has pH values lying in the range of 11–12 [13], and similar trends have been observed for the CO_2-unloaded amine samples for the present experimental work, which is listed in Table B6 of Appendix – B. Initially, the amine's pH decreases very fast with time; however, as time proceeds, this pH-decreasing tendency of the amine blend becomes sluggish because of the reduced CO_2 loading tendency of the aqueous amine blend [77]. Firstly, the pH value of CO_2-unloaded, CO_2-loaded, and CO_2-regenerated samples of 30 wt% MEA was measured, which yielded a pH of 12.53, 8.50, and 10.21, respectively.

There were 40 experimental run sets established, and the pH for CO_2-unloaded, CO_2-loaded, and pH values of a few CO_2-regenerated samples were determined and finally reported. From Table B6 of Appendix – B, it was found that the CO_2-unloaded and CO_2-loaded amine sample's pH lying in the range of 12.04–12.78 and 8.37–9.50, respectively. The lowest value of pH for the CO_2-loaded sample was 8.37, corresponding to run no. 09 (T = 298.15 K, P_{CO2} = 25.33 kPa, m_{HMDA} = 0.20, C = 1 mol/L and α = 1.2174 mol CO_2/mol amine). Likewise, the maximum pH value for the CO_2-loaded amine blend sample

was 9.50, and it was observed in run no. 40 (T = 333.15 K, P_{CO2} = 25.33 kPa, m_{HMDA} = 0.20, and C = 3 mol/L, α = 0.7155 mol CO_2/mol amine). CO_2-loaded amine blend samples with run no. 07, 21, and 34 were regenerated, which led to a final pH of 9.89, 10.51, and 10.54, respectively. The influence of solution concentration on the pH value for CO_2-unloaded, CO_2-loaded, and CO_2-regenerated amine blend samples is shown in Figure 4.3.

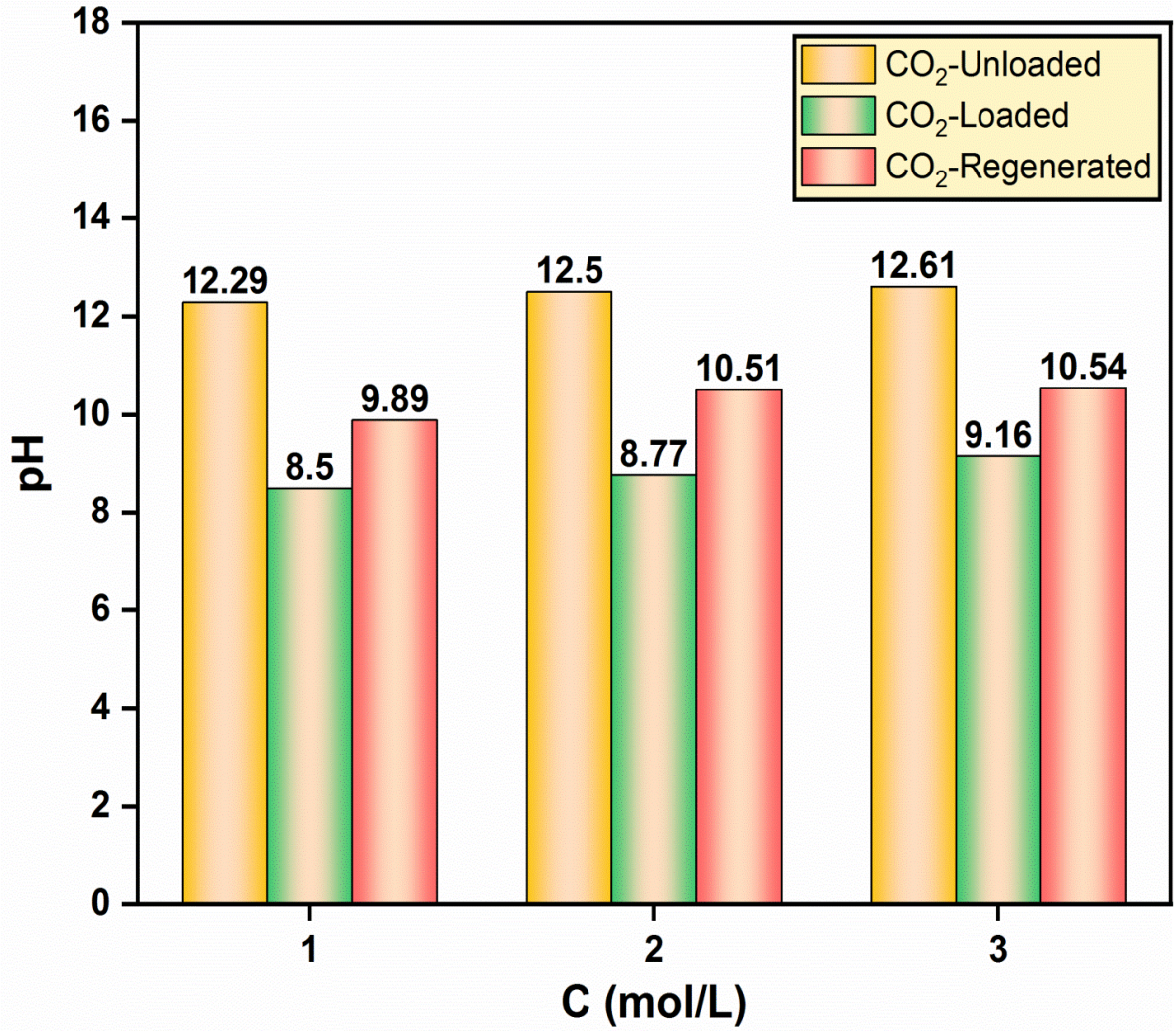

Figure 4.3 Effect of solution concentration, i.e., C = 1, 2, and 3 mol/L on solution pH for CO_2-unloaded, CO_2-loaded, and CO_2-regenerated novel aqueous amine blend of HMDA+DMAE at T = 313.15 K, P_{CO2} = 25.33 kPa, and m_{HMDA} = 0.20.

When solution concentration rose from 1 to 3 mol/L, the pH values for CO_2-unloaded, CO_2-loaded, and CO_2-regenerated amine samples also increased accordingly. During CO_2 absorption experiments, carbamate, bicarbonate, and carbonate ions were formed, resulting in a lowering of solution pH. When the CO_2-loaded HMDA+DMAE amine blend was heated, the bicarbonate and carbonate ions dissociated during regeneration; thus, the captured CO_2 in the amine blend was liberated, and the solution tried to attain its original pH value, but it did not happen so. Therefore, the pH of the CO_2-regenerated samples was minutely lesser than that of CO_2-unloaded amine blends because a percentage of CO_2 was still left over even after regenerating the solution [2]. So, the experimental results show that the regenerated amine samples exhibit a pH lying between 9 to 11.

4.4.5 Thermophysical property: Density estimation

The density estimation for the CO_2-unloaded, CO_2-loaded, and CO_2-regenerated amine blend samples was measured to judge the effect of CO_2 interaction with the novel HMDA+DMAE amine blend. The discussion of this section is based on Table B6 of Appendix – B**;** run no. 09 (T = 298.15 K, P_{CO2} = 25.33 kPa, m_{HMDA} = 0.20 and C = 1 mol/L) provided the maximum α value of 1.2174 mol CO_2/mol amine. Therefore, the density for CO_2-unloaded, CO_2-loaded and CO_2-regenerated amine samples for this experimental run was determined to be $\rho_{unloaded}$ = 995.7 kg/m^3, ρ_{loaded} = 1035.6 kg/m^3, and $\rho_{regenerated}$ = 1011.4 kg/m^3. Similarly, for run no. 40 (T = 333.15 K, P_{CO2} = 25.33 kPa, m_{HMDA} = 0.20 and C = 3 mol/L) in which the minimum α value was achieved i.e., 0.7155 mol CO_2/mol amine, and $\rho_{unloaded}$ = 986.1 kg/m^3, ρ_{loaded} = 1058.8 kg/m^3, and $\rho_{regenerated}$ = 1018.9 kg/m^3. In this chain, run 07 (T = 313.15 K, P_{CO2} = 25.33 kPa, m_{HMDA} = 0.20 and C = 1 mol/L) was used to authenticate the ionic species available in the amine samples by

using characterization techniques of ^{13}C NMR and FTIR; therefore, the density data for this experimental run is as follows: $\rho_{unloaded}$ = 995.5 kg/m^3, ρ_{loaded} = 1031.8 kg/m^3, and $\rho_{regenerated}$ = 1013.6 kg/m^3. $\Delta\alpha$ and cyclic capacity at different operating conditions were evaluated through run no. 07, 21 (T = 313.15 K, P_{CO2} = 25.33 kPa, m_{HMDA} = 0.20, C = 2 mol/L, α = 1.0037 mol CO_2/mol amine, $\rho_{unloaded}$ = 990.6 kg/m^3, ρ_{loaded} = 1056.8 kg/m^3, and $\rho_{regenerated}$ = 1012.0 kg/m^3), and 34 (T = 313.15 K, P_{CO2} = 25.33 kPa, m_{HMDA} = 0.20, C = 3 mol/L, α = 0.8793 mol CO_2/mol amine, $\rho_{unloaded}$ = 989.6 kg/m^3, ρ_{loaded} = 1077.0 kg/m^3, and $\rho_{regenerated}$ = 1015.6 kg/m^3), as discussed in the preceding sections. Now, the influence of enhancing HMDA molar ratio in the novel blend was judged for heat duty and regeneration efficiency. Condition 1st: 0.5 mol/L HMDA–2.5 mol/L DMAE ($\rho_{unloaded}$ = 983.2 kg/m^3, ρ_{loaded} = 1073.7 kg/m^3, and $\rho_{regenerated}$ = 1012.4 kg/m^3), Condition 2nd: 1 mol/L HMDA–2 mol/L DMAE ($\rho_{unloaded}$ = 982.1 kg/m^3, ρ_{loaded} = 1.0808 g/cm^3, and $\rho_{regenerated}$ = 1.0313 g/cm^3), Condition 3rd: 1.5 mol/L HMDA–1.5 mol/L DMAE ($\rho_{unloaded}$ = 977.6 kg/m^3, ρ_{loaded} = 1086.3 kg/m^3, and $\rho_{regenerated}$ = 1035.6 kg/m^3), and Condition 4th: 2 mol/L HMDA–1 mol/L DMAE ($\rho_{unloaded}$ = 975.0 kg/m^3, ρ_{loaded} = 1093.2 kg/m^3, and $\rho_{regenerated}$ = 1045.5 kg/m^3). Finally, density data for 30 wt% MEA is as follows: $\rho_{unloaded}$ = 1008.0 kg/m^3, ρ_{loaded} = 1117.2 kg/m^3, and $\rho_{regenerated}$ = 1075.1 kg/m^3.

Based on the above experimental density data for run no. 07, 21, and 34, it was found that the density for all the CO_2-unloaded amine blend samples was almost similar, and no variation in the density was observed [114]. But, when CO_2 was loaded in the amine sample, the density was increased as compared with CO_2-unloaded samples. According to

the experimental investigation, this density increment was also dependent upon the solution concentration, i.e., when the solution concentration increased from C = 1 mol/L to C = 3 mol/L, the density also enhanced correspondingly. On increasing the solution concentration, amine molecules enhance, which increases the solution's overall mass while the volume remains unaffected; therefore, the solution density also increases [80,115]. On regenerating these solutions, the density of all the solutions decreased, and the density range of these solutions was almost similar but slightly higher than CO_2-unloaded amine solutions. Similar tendencies of the result were seen for all the experiments corresponding to the CO_2-regenerated amine samples. The main reason for this scenario is that when CO_2 gets absorbed in the amine sample, the mass of the solution increases, and the vice-versa effect was encountered in the case of regeneration experiments, but the volume change was negligible. Now, the reason for the higher value of density for CO_2-regenerated amine blends than CO_2-loaded samples lay in the fact that while regenerating the solution, it was impossible to liberate the entire absorbed CO_2 in the novel amine bled, and the reasons have been described in the characterization sections.

4.4.6 Study of ^{13}C NMR results

The spectral analysis of HMDA and DMAE species in the novel HMDA+DMAE amine blend was done by ^{13}C NMR spectroscopy to validate the intermediate products generated chemically reacting with CO_2, as discussed in the previous section of the reaction mechanism. Run no. 07 (T = 313.15 K, P_{CO2} = 25.33 kPa, m_{HMDA} = 0.20, C = 1 mol/L, $pH_{CO2-unloaded}$ = 12.20, $pH_{CO2-loaded}$ = 8.50, and $pH_{CO2-regenerated}$ = 9.89) was selected to evaluate the availability of intermediate complexes in CO_2-unloaded, CO_2-loaded, and CO_2-regenerated amine blends. Figure A7 (a) of Appendix – A represents the NMR

spectroscopic analysis of the CO_2-unloaded sample, and it was found that spectral peaks of DMAE were obtained at 44.32 ppm, 58.86 ppm, and 59.74 ppm. Generally, spectral peaks lying in the range of 44.32–59.74 ppm are due to the availability of DMAE in the HMDA+DMAE blend. Identical tendencies of DMAE peaks were also found in most of the literature [1,40,116]. As DMSO-d_6 was mixed with the amine samples to ensure signal locking, its peak was obtained at 39–41 ppm. Many spectral peaks of varying intensities of HMDA have been obtained at 25.90, 29.58, 30.36, 31.41, 31.58, 37.50, 37.67, 37.84, 38.01, 38.18, 38.35, and 38.52 ppm. The presence of HMDA spectral peaks can generally be represented in the 25.90–38.52 ppm range for CO_2-unloaded amine blend.

On performing the CO_2-absorption experiment, CO_2 chemically reacts with the novel blend, forming carbamate (H_2NCOO^-), bicarbonate (HCO_3^-), and carbonate (CO_3^{2-}). The spectral peaks corresponding to HCO_3^- and CO_3^{2-} species were obtained at chemical shifts of 160.48 ppm**.** Figure A7 (b) of Appendix – A represents the NMR spectroscopic spectral analysis of a CO_2-loaded novel amine blend. In most of the literature, the peak lying anywhere in the range of 160–168 ppm (except the carbonyl region) is mainly responsible because of the formation of HCO_3^- and CO_3^{2-} species [1,40,116]. Huang et al. [65], in their experimental work of ^{13}C NMR chemical species characterization, reported that the peak present in the carbonyl region (i.e., C = O bond) in between 163–165 ppm is mainly responsible for carbamate formation. One peak was discovered at 164.55 ppm for this current experimental work, indicating carbamate formation. The chemical shifts of $HMDAH^+$ and $DMAEH^+$ were discovered in the zone of 25.04–38.49 ppm and 43.19–59.09 ppm, respectively. Compared with the CO_2-unloaded sample, the frequency of chemical shifts of $HMDAH^+$ and $DMAEH^+$ peaks shrink slightly. The formation of the amine-CO_2

product was the primary cause of spectral peak shrinkage in the CO_2-loaded amine blend sample [7].

CO_2 liberates during desorption experiments by dissociating HCO_3^-/CO_3^{2-} species due to the supply of external heat to the regeneration reactor. The desorption experiments were conducted over different operating conditions to judge the effectiveness of the novel blend. Figure A7 (c) of Appendix – A represents the NMR spectroscopic spectral analysis of a CO_2-regenerated novel amine blend. NMR spectra reveal that the peaks of HMDA and DMAE species were obtained at 25.25–38.64 ppm and 44.06–59.62 ppm range, respectively. It was a clear indication that slight shrinkage in the chemical shifts due to the amine-CO_2 product, as observed in the CO_2-loaded sample, again returned their near original values, as in the case of CO_2-unloaded amine blend samples. NMR investigation of CO_2-regenerated sample, carbamate and HCO_3^-/CO_3^{2-} species were still present at 164.37 ppm and 160.65 ppm, respectively. But HCO_3^-/CO_3^{2-} species intensity was diminished as compared with the CO_2-loaded amine sample. It indicates that the availability of such species in the amine sample was reduced to a large extent (i.e., easily decomposable) due to heat supplied. At the same time, the intensity of carbamate remained unaffected because it is pretty challenging to decompose such species. Zhao et al. [7] discovered a similar trend of results corresponding to the NMR characterization of CO_2-regenerated amine in their investigation. The spectral peaks of DMSO-d_6 remained unaffected in all cases. Table B9 of Appendix – B shows the availability of intermediate chemical species and their spectral range that exist in CO_2-unloaded, CO_2-loaded, and CO_2-regenerated novel HMDA+DMAE amine blend.

4.4.7 Study of FTIR results

As previously stated, HMDA is a diamine, and DMAE is a tertiary amine in the novel HMDA+DMAE amine blend. Therefore, the characteristic peaks at 3416.02, 3424.51, and 3422.72 cm^{-1} corresponding to CO_2-unloaded, CO_2-loaded, and CO_2-regenerated amine blend samples signify the presence of HMDA, as shown in Figure A8 of Appendix – A. These peaks appeared because of N–H stretching vibration within the HMDA molecules. However, due to the N–H bending of HMDA, the peaks lying at 1571.27, 1647.87, and 1628.87 cm^{-1} were also responsible for HMDA corresponding to CO_2-unloaded, CO_2-loaded, and CO_2-regenerated amine blend samples. Vibration due to C–N stretching of HMDA was found at the characteristic peaks of 1047.64, 1013.73, and 1023.81 cm^{-1}, corresponding to CO_2-unloaded, CO_2-loaded, and CO_2-regenerated amine blend samples. Nandiyanto et al. [87] confirmed a similar trend of peaks caused by N–H stretching, C–N stretching, and N–H bending of primary amine, i.e., HMDA. The primary and secondary amines also exhibit a broad N–H wag band, with characteristic peaks located between 665–910 cm^{-1}. One peak at 820.39 cm^{-1} for the CO_2-unloaded sample, two peaks at 837.28 and 696.75 cm^{-1} for the CO_2-loaded sample, and again two peaks at 837.25 and 696.14 cm^{-1} for the CO_2-regenerated samples were obtained due to N–H wag of HMDA.

In the case of tertiary amines, N–H stretching and N–H wag vibrations are absent; therefore, only C–N stretching can be found in DMAE. One characteristic peak at 499.94 cm^{-1} for CO_2-unloaded, two peaks at 499.99 and 645.27 cm^{-1} for CO_2-loaded, and two peaks at 499.93 and 586.16 cm^{-1} for CO_2-regenerated samples were attained because of the DMAE availability in the novel amine blend. Similarly, peaks for all samples of amine blends lying between the wavenumber of 2800–2950 cm^{-1} and 1000–1250 cm^{-1} were

responsible for C–N stretching of DMAE, as shown in Figure A8 of Appendix – A. Stretching vibration due to $C = O$ bond due to DMAE was found in the frequency range of 1380–1485 cm^{-1} [117].

Carbamate, carbonate, and bicarbonates were formed upon the successful CO_2 loading in the amine samples. NH_2^+ deformation is mainly responsible for amine protonation and carbonate species formation [36]. The availability of asymmetric carbonyl ($-COO^-$) stretching vibration at characteristic peaks of 1283.38, 1628.74, and 1697.79 cm^{-1} for CO_2-loaded and 1297.63, 1565.30, and 1697.63 cm^{-1} for CO_2-regenerated amine blend samples was present due to the formation of carbamate [17,25,36,63,117]. Interaction between the hydroxyl group of tertiary amine and CO_2 is responsible for the carbamate formation, which was absent in the CO_2-unloaded samples [118]. Carbamate peaks were still present in the regenerated amine blend samples because such bonds were difficult to break when the heat was supplied during regeneration.

4.4.8 Heat duty and regeneration efficiency results

The external heat needed to regenerate the CO_2-loaded aqueous amine blend solution is a critical aspect that must be determined during desorption experiments for evaluating the effectiveness of the amine blend; therefore, the external requirement of heat is referred to as heat duty [2,24,31,44,76,113]. For estimating the heat duty for the novel HMDA+DMAE amine blend, heat duty data of 30 wt% MEA was acquired from the investigation performed by Narku-Tetteh et al. [44]. According to the researchers, the heat duty needed to regenerate the 30 wt% MEA was 450 kJ/mol CO_2, so this data was chosen as a standard reference for further investigations. Upon successful CO_2 loading in the MEA solution, more stable carbamate was formed; therefore, while regenerating, it requires high heat duty

[24]. The heat transfer value, when calculated by Eq. 4.5, remains unchanged for the entire experimental work. Therefore, cyclic capacity became more prominent in determining heat duty value, which is inversely related to cyclic capacity. Experimental investigation on cyclic capacity for novel HMDA+DMAE amine blend corresponding to solution concentration follows the trend: 3 mol/L > 2 mol/L > 1 mol/L [1,2].The relationship between heat duty and different solution concentrations, i.e., C = 1, 2, and 3 mol/L, along with conventional 30 wt% MEA, is shown in Figure 4.4 (a).

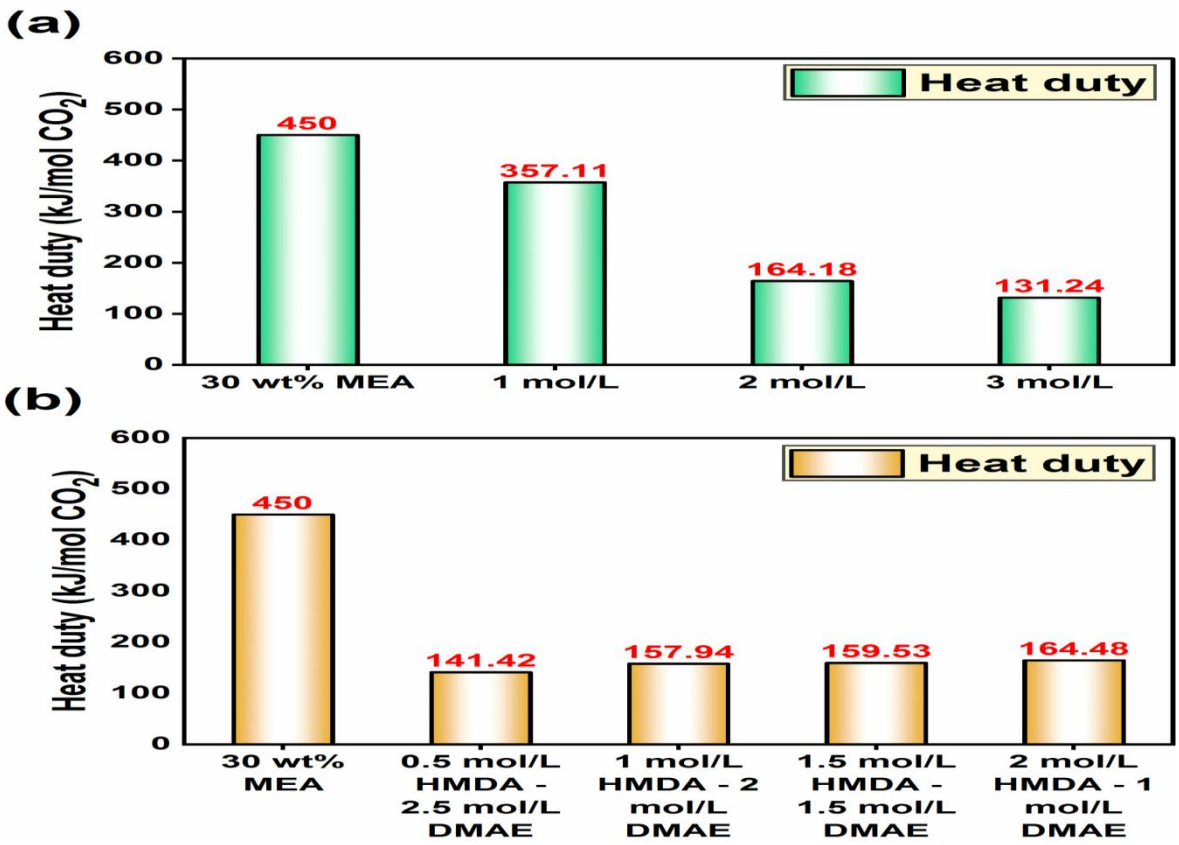

Figure 4.4 The correlation between solution concentration and molar ratio of HMDA on heat duty; (a) comparison between the heat duty values for 30 wt% MEA and solution concentration, i.e., C = 1, 2, and 3 mol/L for the novel aqueous amine blend of HMDA+DMAE for post-combustion CO_2 capture; (b) Effect of increasing the HMDA molar ratio in the novel aqueous amine blend of HMDA+DMAE on heat duty at T = 313.15 K, P_{CO2} = 25.33 kPa, and C = 3 mol/L.

It was discovered that 357.11, 164.18, and 131.24 kJ/mol CO_2 heat duty was experimentally determined, corresponding to C = 1, 2, and 3 mol/L, respectively. On comparing with 30 wt% MEA, a reduction in heat duty of 20.64 %, 63.51 %, and 70.83 % was achieved, corresponding to C = 1, 2, and 3 mol/L, respectively. Now, examining the influence of the molar ratio of HMDA (i.e., activator) in the novel aqueous HMDA+DMAE amine blend on heat duty assessment was mandatory. Therefore, four different CO_2 absorption experiments were done to judge the molar ratio of the HMDA effect on heat duty. Operating conditions, Experiment 1st: 0.50 mol/L HMDA–2.50 mol/L DMAE (T = 313.15 K, P_{CO2} = 25.33 kPa, m_{HMDA} = 0.166, C = 3 mol/L, α = 0.8784 mol CO_2/mol amine); Experiment 2nd: 1 mol/L HMDA–2 mol/L DMAE (T = 313.15 K, P_{CO2} = 25.33 kPa, m_{HMDA} = 0.333, C = 3 mol/L, α = 0.9723 mol CO_2/mol amine); Experiment 3rd: 1.50 mol/L HMDA–1.50 mol/L DMAE (T = 313.15 K, P_{CO2} = 25.33 kPa, m_{HMDA} = 0.50, C = 3 mol/L, α = 1.0456 mol CO_2/mol amine); and Experiment 4th: 2 mol/L HMDA–1 mol/L DMAE (T = 313.15 K, P_{CO2} = 25.33 kPa, m_{HMDA} = 0.667, C = 3 mol/L, α = 1.1782 mol CO_2/mol amine). The effect of enhancing the HMDA molar ratio in the novel aqueous amine blend of HMDA+DMAE on heat duty is shown in Figure 4.4 (b). It was found that on enhancing the value of HMDA in an amine solution, the value of heat duty of regeneration also increased accordingly. This research finding was also validated by the previous investigations performed by Gautam and Mondal [2], Wai et al. [76], and Muchan et al. [24]. When the HMDA molar ratio is enhanced in the HMDA+DMAE amine blend, the ΔH_{abs} value and HCO_3^- ion formation increase; as a result, large heat would be needed to regenerate the amine blends. Based on the above discussion, the trend of enhancing molar ratio of HMDA in novel amine blend of HMDA+DMAE on heat duty is as follows:

30 wt% MEA > 2 mol/L HMDA–1 mol/L DMAE > 1.50 mol/L HMDA–1.50 mol/L DMAE > 1 mol/L HMDA–2 mol/L DMAE > 0.50 mol/L HMDA–2.50 mol/L DMAE. To evaluate the performance of any novel aqueous amine blend, regeneration efficiency is another important aspect that must be targeted. The regeneration efficiency for the novel aqueous HMDA+DMAE amine blend for run no. 07, 21, and 34 was found to be 52.21 %, 63.51 %, and 60.47 %, respectively. The regeneration efficiency for 30 wt% MEA was estimated to be 31.23 %. According to these experimental data, it is conferred that this novel amine blend performed well in terms of regeneration efficiency, which was approximately twice as efficient as 30 wt% MEA.

4.4.9 Investigation of CO_2 absorption and desorption rates

The initial CO_2 absorption rate was calculated for increasing HMDA molar ratio in the novel HMDA+DMAE amine blend, i.e., 0.5 mol/L HMDA–2.5 mol/L DMAE, 1 mol/L HMDA–2 mol/L DMAE, 1.5 mol/L HMDA–1.5 mol/L DMAE and 2 mol/L HMDA–1 mol/L DMAE and the experiments were done at T = 313.15 K, P_{CO2} = 25.33 kPa, and C = 3 mol/L. The influence of the molar ratio of HMDA on the initial absorption rate was estimated according to the operating condition, as discussed above, and the same is shown in Figure 4.5 (a). The experimental values of the CO_2 absorption rate were compared with 30 wt% MEA solution at the same operating parameters. It was observed that on escalating the HMDA molar ratio in the novel aqueous HMDA+DMAE amine blend, the CO_2 absorption rate was also enhanced.

For 30 wt% MEA, the initial CO_2 absorption rate was calculated to be 16×10^{-4} mol CO_2/(L solution. min). In this sequence, the order of CO_2 absorption rate for the novel HMDA+DMAE amine blend is as follows: 0.5 mol/L HMDA–2.5 mol/L DMAE < 1 mol/L

HMDA–2 mol/L DMAE < 1.5 mol/L HMDA–1.5 mol/L DMAE < 2 mol/L HMDA–1 mol/L DMAE. When the molar ratio of HMDA to DMAE is 0.20, the absorption rate was slower than 30 wt% MEA. In the case of 0.50 molar ratio, the rate of CO_2 absorption of the novel blend was comparable with MEA, while in the rest of the cases, the absorption rate was faster than MEA. The main reason for this scenario is that enhancing the HMDA molar ratio in the HMDA+DMAE amine blend causes higher CO_2 gas molecule interaction because of the availability of two primary amino groups in the HMDA's molecular structure [31,76]. Wai et al. [31] prepared an amine blend of AMP+DETA and varied the activator's molar ratio, i.e., DETA in the amine blend, and it was found that on enhancing the DETA molar ratio, the absorption rate was also increased; therefore, their investigation validated the present experimental research findings of the CO_2 absorption rate. Kumar and Mondal [15] prepared the amine blend of 2-(Diethylamino)ethanol (DEEA) with various diamines, i.e., PZ, HMDA, 2-(2-Aminoethylamino)ethanol (AEEA), Ethylenediamine (EDA), and 3-(Dimethylamino)-1-propylamine (DMAPA). Their research found that HMDA+DEEA beat other diamines regarding CO_2 absorption rate. The experimental study disclosed that the CO_2 absorption rate was faster initially and became sluggish as time progressed [14]. Solvents with high initial CO_2 absorption rates are always advantageous over other solvents in terms of an economic point of view [4]. In this work, the initial CO_2 absorption rate for 2 mol/L HMDA–1 mol/L DMAE was 26×10^{-4} mol CO_2/(L solution. min), which yielded a 62.5% higher absorption rate than 30 wt% MEA. This novel amine blend's high CO_2 absorption rate is highly economical and can lower overall operational costs [6].

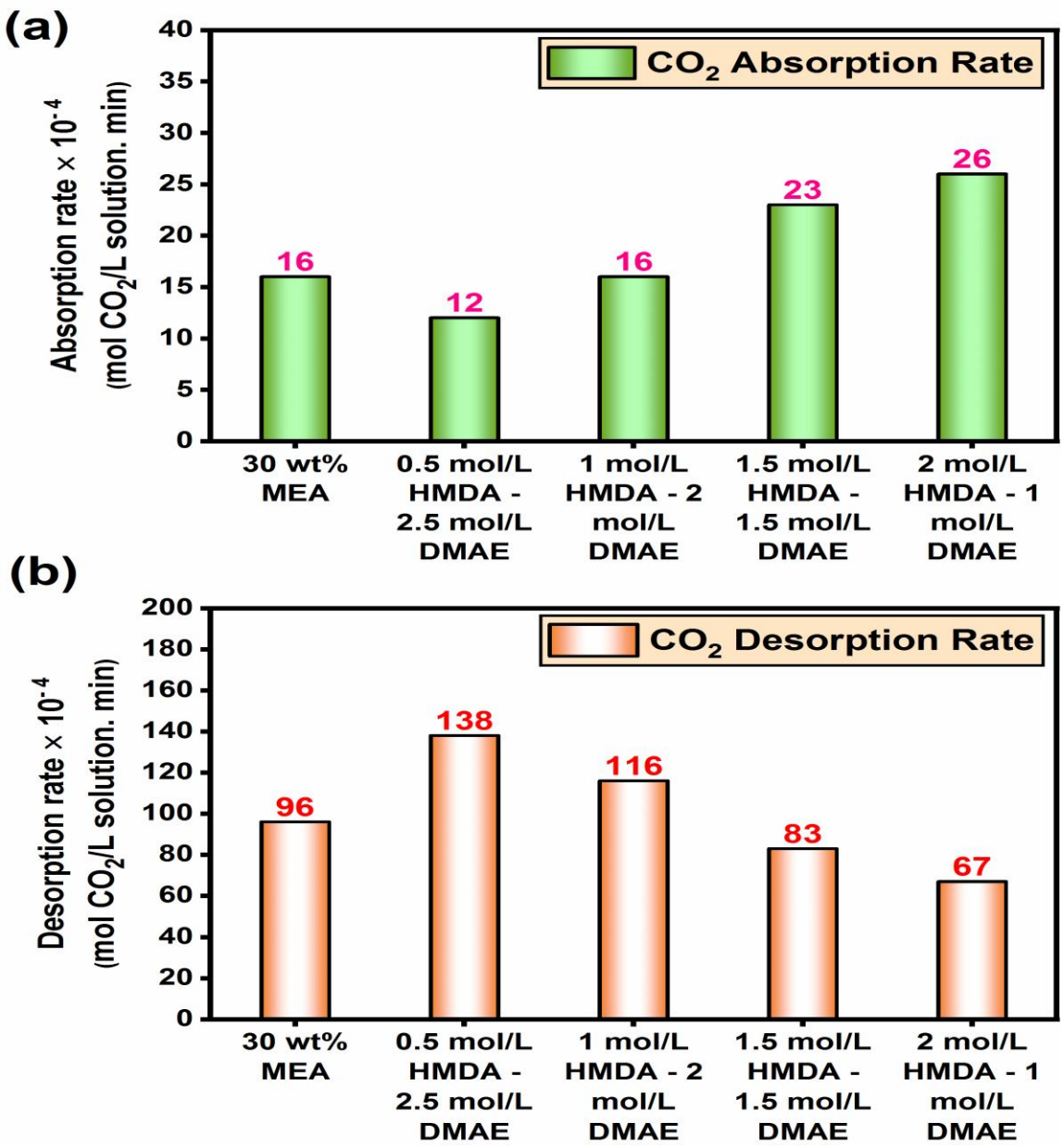

Figure 4.5 (a) Effect of increasing molar ratio of HMDA in the novel aqueous amine blend of HMDA+DMAE on the initial absorption rate; (b) Effect of increasing molar ratio of HMDA in the novel aqueous amine blend of HMDA+DMAE on the initial desorption rate.

Similarly, the CO_2 desorption rates were also examined for the similar increasing composition of HMDA in the HMDA+DMAE amine blend, as discussed above. The CO_2 absorption and desorption rates are two opposing processes [31]. The relationship between different molar ratios of HMDA in the amine blend of HMDA+DMAE and 30 wt% MEA corresponding to the initial desorption rate is shown in Figure 4.5 (b). This investigation revealed that 30 wt% MEA has a desorption rate of 96×10^{-4} mol CO_2/(L solution. min). The experimental trend of desorption rate on enhancing the HMDA molar ratio is as follows: 0.5 mol/L HMDA–2.5 mol/L DMAE > 1 mol/L HMDA–2 mol/L DMAE > 1.5 mol/L HMDA–1.5 mol/L DMAE > 2 mol/L HMDA–1 mol/L DMAE. When the molar ratios of HMDA to DMAE were 0.20 and 0.5, the desorption rate was higher than 30 wt% MEA, and for the remaining cases, it was lower. The experimental investigation also revealed that the desorption results were increased by decreasing the HMDA molar ratio in the novel amine blend from 2 to 0.20. The main reason for this situation was because of enhancing HMDA molar ratio in the amine blend, the concentration of DMAE reduced, which ultimately reduced the concentration of HCO_3^- ions due to DMAE. Zhang et al. [4], He et al. [6] and Shi et al. [33] explained the influence of the presence of HCO_3^- ion on the desorption process, and in their investigation, they reported that when large moles of HCO_3^- ions are present in any amine blend system than it will be easy to enhance the deprotonation of protonated amine ($Amine - H^+$). Since the decomposition efficiency of the HCO_3^- ion is higher than that of carbamate ions [6]. While reacting with the HCO_3^- ions, the protonated amines form the carbonic acid (H_2CO_3) and further dissociate into CO_2 and H_2O [Eq. 4.31 and Eq. 4.32].

$$AmineH^+ + HCO_3^- \leftrightarrow Amine + H_2CO_3 \quad (4.31)$$

$$H_2CO_3 \leftrightarrow H_2O + CO_2 \quad (4.32)$$

When protonated amines react with H_2O, deprotonated amines are formed, but this is a very slow path of reaction since the pH of H_2O is lower than HCO_3^- [Eq. 4.33].

$$AmineH^+ + H_2O \leftrightarrow Amine + H_3O^+ \quad (4.33)$$

The CO_2 desorption rate for the present experimental work was also validated by the investigation performed by Wai et al. [31]. Based on the discussion, it was encountered that the initial CO_2 desorption rate of 0.5 mol/L HMDA–2.5 mol/L DMAE was 43.75 % higher than the benchmark 30 wt% MEA.

4.4.10 Study of ΔH_{abs} results

In this present study, the estimation of ΔH_{abs} value for the novel HMDA+DMAE amine blend was done by adopting the Gibbs–Helmholtz equation because most of the researchers relied on and calculated ΔH_{abs} value by using this equation [1,2,91,93]. ΔH_{abs} value for any amine solvent gives information about the kinetic performance of that solvent [13]. By equilibrium CO_2 loading data, as represented in Table B6 of Appendix – B, a few experimental run sets yielded approximately similar equilibrium CO_2 loading. Therefore, in this scenario of nearly constant equilibrium CO_2 loading, i.e., α = 1.00 and α = 1.07 mol CO_2/mol amine, different sets of T and P_{CO2} values were chosen. A plot between $\frac{1}{T}$ (X-axis) and $\ln P_{CO2}$ (Y-axis) was drawn at the aforementioned condition, and the same has been shown in Figure 4.6. Based on these plots, two different trend lines were drawn with slopes –9088.8 and –9074.4 at constant α = 1.07 and 1.00 mol CO_2/mol amine, respectively. When the universal gas constant is multiplied by slopes, trend lines result in ΔH_{abs} value, i.e., –75.56 kJ/mol and –75.44 kJ/mol. Therefore, the final average ΔH_{abs} value for the novel HMDA+DMAE amine blend was determined to be –75.50 kJ/mol. According to this

investigation, it is concluded that the ΔH_{abs} value for the current novel blend is lower than traditional primary MEA (ΔH_{abs} = –85.13 kJ/mol) [46] but higher than conventional tertiary amine MDEA (ΔH_{abs} = –54.60 kJ/mol) [89].

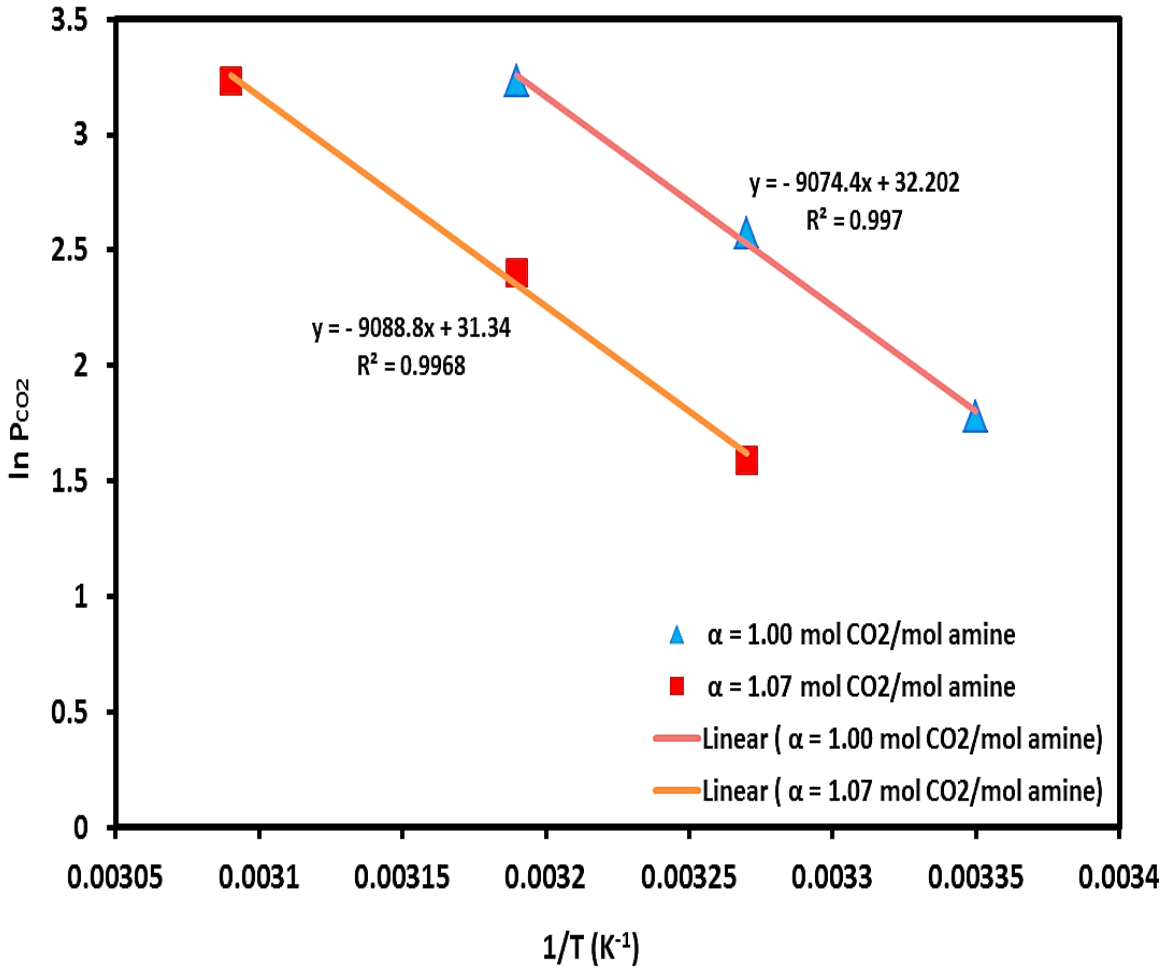

Figure 4.6 Plot in between ln P_{CO2} and 1/T for two different sets of equilibrium CO_2 loading i.e., α = 1.00 and α = 1.07 mol CO_2/mol amine for the estimation of ΔH_{abs} for the novel aqueous amine blend of HMDA+DMAE for post-combustion CO_2 capture.

4.4.11 Response surface methodology (RSM) – a statistical tool for optimization

Box and Wilson, in 1951 introduced the concept of RSM to enhance the production of the chemical industries [119,120]. RSM is a robust multivariable statistical technique for solving all real-life engineering and non-engineering problems by creating experimental run sets at pre-defined operating conditions [1,2,69,70,121,122]. RSM approach is used in modeling to fit the model equation developed by this software corresponding to experimental results [70,71,123,124]. The correlation between the independent and dependent variables can be expressed as [2]:

$$Y = f(X_1,\ X_2,\ X_3, \dots\dots\dots\dots,\ X_N) + \omega \quad (4.34)$$

Where Y is the final response of the system (i.e., Dependent variables); X_1, X_2, X_3,……, X_N are the factors (i.e., Independent variables); and ω denotes the error function for the chosen system.

The quadratic model is highly trustworthy, and its generalized equation in the form of a polynomial can be represented as [115,119,121]:

$$Y = \tau_0 + \sum_{i=1}^{n} \tau_i x_i + \sum_{i=1}^{n} \tau_{ii} x_i^2 + \sum_{i=1}^{n} \sum_{j>1}^{n} \tau_{ij} x_i x_j + \omega \quad (4.35)$$

Where Y represents the ultimate response, τ_0 signifies the constant coefficient, τ_i represents the linear constant coefficient, τ_{ii} denotes the quadratic constant coefficients, τ_{ij} signifies the mutual interaction coefficients, and ω denotes random error. At last, X_i and X_j are the independent variables in the coded manner for the particular system. The detailed description of the RSM approach has already been discussed in section 3.4.11 of Chapter 3.

4.4.11.1 Algorithm for implementing RSM for the novel HMDA+DMAE amine blend

The RSM approach has been applied to the present work in which the novel aqueous HMDA+DMAE amine blend was used for CO_2 capture. Under specified operating

conditions, the RSM optimization technique aided in achieving the best possible result, i.e., equilibrium CO_2 loading. An algorithm employing RSM for modeling and optimizing experimental work can easily be understood in 10 simple steps. This step-by-step procedure for implementing this statistical technique is shown in Figure A9 of Appendix – A. The step procedure for implementing RSM has been incorporated in the B10 of Appendix – B.

4.4.11.2 RSM implementation in the present experimental work

In this experimental work, the prime objective is to optimize the α value corresponding to all the factors involved in the entire system. T, P_{CO2}, m_{HMDA}, and C were the four factors that influenced the α value. The lower and upper limits of such factors are as follows: T = 298.15–333.15 K, P_{CO2} = 10.13–25.33 kPa, m_{HMDA} = 0.05–0.20, and C = 1–3 mol/L. Stat-Ease created Design-Expert® software, and its 8.0.6 trial version was employed to design the various run sets; further, experimental work was optimized by adopting the CCD. According to the assigned range of independent variables (i.e., factors), the RSM software created 30 sets of experiments consisting of 16 factorial points, 8 axial points, and 6 central points. Therefore, in a set of 30 experimental runs, 24 non-central, and 6 central points exist. The information about the entire experimental runs involved in any system can be understood as follows:

$$N = 2^n + 2n + n_c = (2)^4 + 2(4) + 6 = 30 \quad (4.36)$$

Where N denotes the total no. of runs produced by the RSM; n signifies the factors included in the experimental work; and n_c is the central points.

The quadratic model was selected among the various available models in the RSM software because it provides reliable results. Based on all the descriptions, it can be finally concluded that the RSM software with the CCD approach and quadratic model aided in

forming 30 experimental runs. The software-generated experimental sets can be performed in any order, and no specific rule exists regarding the experimental order. Therefore, in this current experimental work, the sequence of experiments remains the same as developed by the RSM software. According to RSM-generated run sets, actual experiments were done in the laboratory. The α values were estimated, and their values were inserted in each column in the response section of the experimental run sheet that was generated by RSM software. After assigning every response to the software, the RSM software analyzed the experimental data and correspondingly developed an empirical model in the form of a polynomial equation [124].

4.4.11.3 Experimental investigation of RSM study

The prime task of this present experimental work was to optimize α value for the novel aqueous HMDA+DMAE amine blend by using the RSM approach. The experimental investigations were performed on the same order of run sets as developed by the RSM software, and the experiments were done under pre-defined operating conditions. The independent variables like T, P_{CO2}, m_{HMDA}, and C were assigned codes as A (i.e., T = 298.15–333.15 K), B (i.e., P_{CO2} = 10.15–25.33 kPa), C (i.e., m_{HMDA} = 0.05–0.20), and D (i.e., C = 1–3 mol/L), respectively. RSM software coded the factors in terms of $\pm$ α, $\pm$ 1 and 0 (mean value), and such information was obtained from the design summary section within the RSM software; therefore, the information regarding the coded level is shown in Table B11 of Appendix – B. Depending on the operating condition, RSM's generated experimental run sets, and these run sets have various combinations of independent variables, point type (i.e., axial, central, and factorial), cook's distance, and their final response (Y), and the same has been shown in Table B12 of Appendix – B.

Cook's distance is a critical aspect in validating the second-order quadratic model by providing information about any error in the experimental data. Cook's distance estimation is the most significant way to judge the correctness and reliability of the experiments. The value of the cook's distance must lie between 0 and 1, and any such system whose cook's distance value is outside this range is identified as a system without an outlier [2,68]. The presence of an outlier always influences the model's accuracy and reliability; therefore, an outlier must not be present in any system. The experimental investigation for the novel aqueous HMDA+DMAE blend revealed that the value of the cook's distance for every 30 experimental run sets lay in the range of 0 and 1. Therefore, the cook's distance for this present system clearly indicates that the chosen quadratic model is highly reliable and accurate. In 30 experimental runs, the run no. 24 was identified as a factorial point that had a cook's distance of 0.088, and it showed a maximum α value of 1.0586 mol CO_2/mol amine at T = 306.90 K, P_{CO2} = 21.53 kPa, m_{HMDA} = 0.16, and C = 1.50 mol/L. In this sequence, run no. 20 (i.e., factorial point with cook's distance = 0.050) acquired the minimum α value of 0.6054 mol CO_2/mol amine at T = 324.40 K, P_{CO2} = 13.93 kPa, m_{HMDA} = 0.09, and C = 2.50 mol/L.

4.4.11.4 Establishing the relationship between the factors and the final response

RSM software develops a model, and that model correlates different independent variables with the final response (Y), i.e., α value. Figure 4.7 (a), (b), (c), and (d) indicates the number of experiments resulting a unique α value corresponding to different values of T, P_{CO2}, m_{HMDA}, and C, respectively. Figure 4.7 shows a relationship between response (Y) and temperature, CO_2 partial pressure, mole fraction of HMDA, and solution concentration. Similarly, the relationship between the run sets developed by RSM software and its

corresponding response (Y) has been represented in Table B12 of Appendix – B. As discussed in section 4.4.2, an empirical model was formed that correlated the independent and dependent variables. Based on independent factors, the value of calculated equilibrium CO_2 loading (α_{cal}) as a final response Y was estimated by Eq. 4.28. The values of unknown coefficients were calculated with the help of Microsoft Excel solver, and the values of such coefficients are tabulated in Table B13 of Appendix – B. Now, the % ARD of sets of experimental runs as developed by RSM software was evaluated by Eq. 4.29, and finally, % AARD for the entire 30 experimental runs was calculated by Eq. 4.30, and it was determined to be 2.00 %, which is an outstanding and reliable result coming under 10 % range.

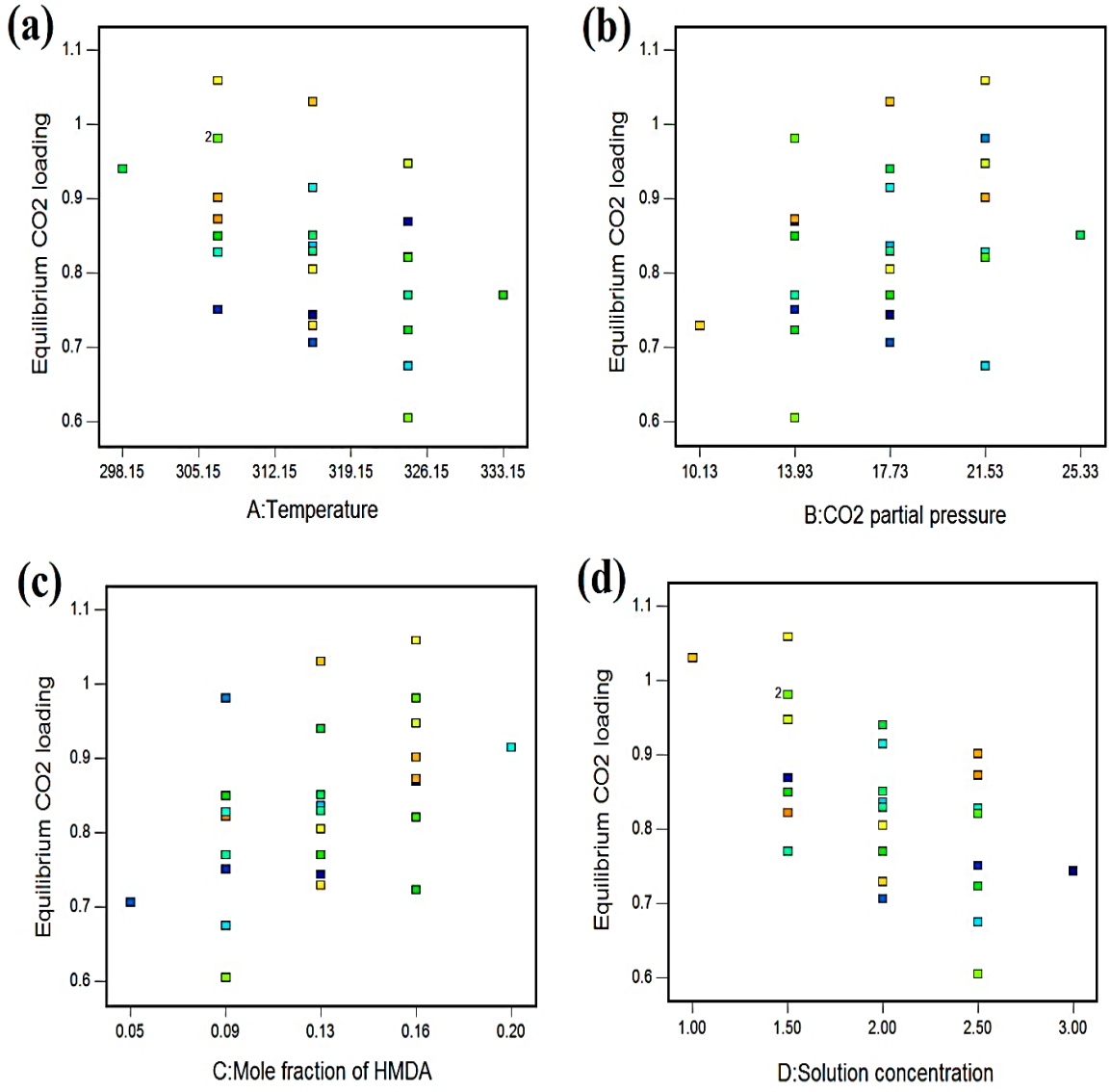

Figure 4.7 Plot of run points correlating factors with equilibrium CO_2 loading as a final response (Y): (a) Temperature (A) vs. Y; (b) CO_2 partial pressure (B) vs. Y; (c) Mole fraction of HMDA (C) vs. Y; (d) Solution concentration (D) vs. Y.

4.4.11.5 Authentication of an empirical model by RSM-CCD approach

As in section 4.4.2, an empirical model was developed based on independent variables, and a Microsoft Excel solver aided in evaluating the values of unknown coefficients. After assessing these unknown coefficients, the calculated values of equilibrium CO_2 loading (α_{cal}) were also determined by using Eq. 4.28. RSM software also predicted the α value according to the designed experimental run sets. In the diagnostics section of the RSM software, a report was generated by the software consisting of predicted values, residuals, leverage, internally studentized residuals, externally studentized residuals, cook's distance, and run order. The developed empirical model was authenticated by comparing the α value obtained by the empirical model and the prediction made by the RSM-CCD approach. It was encountered that the α_{cal} value and the predicted response value closely resemble each other. Therefore, it is concluded that the developed empirical model equation is highly reliable and is suitable for calculating the α values.

4.4.11.6 Selection of quadratic model and its authentication

In order to evaluate the desired final response, it is always mandatory to select an appropriate model; therefore, a quadratic model was selected for estimating the α value for the novel HMDA+DMAE amine blend. In the evaluation part of the RSM software, when the quadratic model was chosen, then standard error, variance inflation factor (VIF), R-squared value, 0.5 standard deviation, 1 standard deviation, and 2 standard deviation terms were encountered. The four factors A, B, C, and D were regarded as factors, and their various combinations were known as terms. These terms were A, B, C, D, AB, AC, AD, BC, BD, CD, A^2, B^2, C^2, and D^2. The standard error value must be similar for similar factors involved in the system, and their smaller value is always better. The standard error

for the terms A to D was 0.20, for AB to CD was 0.25, and A^2 to D^2 was 0.19. VIF measures the multi-collinearity of the regression analysis, and its ideal value is 1, but a value higher than 10 causes alarm to the system [2]. For this work, the VIF value occurs in the range of 1.00–1.05. For A to D and AB to CD terms, the VIF value was 1.00, and for similar interaction terms, i.e., A^2 to D^2, the VIF value was 1.05. Now, the ideal R-squared value for any system must be 0.00, and a higher value indicates high interaction between the factors, and such a condition is a clear indication of a poor selection of the model. For this work, the ideal R-squared value for the terms A to D and AB to CD was 0.00, but for the A^2 to D^2 terms, it was 0.0476. According to standard error, VIF value, and ideal R-squared value, it is concluded that the selection of the quadratic model is highly reliable and accurate, and RSM software has recommended the same.

4.4.11.7 Study of ANOVA results

After providing input data to the RSM software, the analysis process came into the picture, and there were options like transform, fit summary, model, ANOVA, diagnostics, and model graphs were present. When the maximum to minimum response ratio is greater than 10, it needs transformation, but no transformation is necessary for values less than 3. In this present work, the maximum and minimum α value was found to be 1.0586 and 0.6054; the ratio of these values was 1.7486; therefore, no transformation was required. The RSM software recommended that a quadratic model be used, as reported by the fit summary section, but the cubic model and the models with higher orders were not recommended. In the model section, quadratic process order was chosen for further investigation.

Now, it is vital to target ANOVA results to analyze the chosen model's reliability and model quality [2,68]. Table B14 of Appendix – B denotes the ANOVA results of the final response for the novel HMDA+DMAE amine blend. The ANOVA provides knowledge about the interaction among the factors of the system. A sum of squares, degree of freedom (df), mean square, F-value, and p-value are essential parameters on which the ANOVA investigation is dependent [1]. It is well known that when the value of 'Prob > F' is less than 0.0500, then the model terms involved in the system are significant; for the current scenario, the value of Prob > F was found to be < 0.0001. It means that the interaction terms, i.e., A, B, C, D, B^2, and D^2, were the model terms that were significant. The RSM software also suggested that the value of 'Prob > F' terms when greater than 0.1000, the model terms are considered insignificant. The F-value of the model is also a strong basis that suggests whether the selected model is significant or not. It was significant for this experimental work, with a value of 52.37. For the success of the model, the lack-of-fit for the F-value must be insignificant, and for the current work, it was insignificant, with a value of 4.35. A significant lack-of-fit for the F-value is regarded as bad; in that case, it is critical to fit the model [2].

Table 4.3 shows the statistical parameters present in the RSM analysis. These parameters involve standard deviation, mean, coefficient of variance % (C.V. %), PRESS value, R-squared value, adjusted R-squared value, predicted R-squared value, and adequate precision. Amongst all such parameters, the R-squared value and adjusted R-squared value are very important to judge the model's fitness for the regression line. For best and authentic results, the values of R-squared and adjusted R-squared must be close to 1 [1,2,69]. In this sequence, the information about the prediction made by the regression

model is accomplished by the predicted R-squared value [69]. For this experimental work, the value of standard deviation, mean, coefficient of variance % (C.V. %), PRESS value, R-squared value, adjusted R-squared value, and predicted R-squared values were found to be 0.020, 0.84, 2.44, 0.033, 0.9800, 0.9612, and 0.8935. The R-squared and adjusted R-squared values were much closer to 1, and their difference was 0.0677, indicating their reasonable agreement. Adequate precision computes the signal-to-noise ratio, and a ratio higher than 4 is always preferred; for this work, it is 29.831, which indicates the signal's adequacy. The standard error to mean value ratio is known as C.V. %, and it is nothing but the model's reproducibility, which is expressed in percentage [68]. C.V. % value must be less than 10 for the reproducible system, and for the present work, it was found to be 2.44

%. On the basis of the aforementioned process parameters of the ANOVA study, it is finally concluded that the chosen CCD and quadratic model is highly accurate and can be used for further investigations.

Table 4.3 Statistical parameters involved in the ANOVA results for the modelling of equilibrium CO_2 loading as a final response.

Standard deviation	0.020
Mean	0.84
C.V. %	2.44
PRESS	0.033
R-squared	0.9800
Adj R-squared	0.9612
Pred R-square	0.8935
Adeq precision	29.831

4.4.11.8 Experimental modeling by RSM–CCD approach

The RSM software has developed a modeling equation correlating the final response (Y) with all the independent factors present in the system. The final modeling equation can be represented as:

$$\text{Equilibrium } CO_2 \text{ loading (Y)} = 0.83 - 0.055\,A + 0.036\,B + 0.054\,C - 0.070\,D - 0.001075\,AB + 0.005212\,AC - 0.004262\,AD - 0.002875\,BC - 0.0041\,BD + 0.001512\,CD + 0.007731\,A^2 - 0.008594\,B^2 - 0.003506\,C^2 + 0.016\,D^2 \quad (4.37)$$

In this developed model equation, the terms A, B, C, and D were the factors coded for T, P_{CO2}, m_{HMDA}, and C, respectively. Eq. 4.37 denotes the dependency of the final response on the factors and their different interactions involved in the system. Figure 4.8 (a) represents the correlation between the actual values and the predicted final response (Y) value. RSM–CCD, with a quadratic model, made very accurate predictions of various experimental run sets. Therefore, a strong relation between the actual and predicted values was established and plotted along a straight line. Figure 4.8 (b) represents the relationship between the internally studentized residuals and normal % probability for the experimental results of a novel HMDA+DMAE amine blend. The Normal plot of residuals checks the adequacy of the selected model and the distribution of residuals [2,119]. The normal plot of residuals is a graphical representation of a plot drawn between internally studentized residuals (X-axis) and the normal % probability (Y-axis). Residuals are nothing but the difference in predicted and actual experimental values calculated through independent variables involved in the system [1,2,68]. The distribution of the residuals lying in a straight line tells about the normal distribution of errors [68,69]. Studentized residual is a way of reporting residuals, and it is nothing but the residuals to the standard deviation ratio.

Residuals are always distributed along a straight line, and any deviation indicates deflection from the normality [119]. Some scattering of residuals along the straight line is always expected, but it is always assumed that the experimental data is distributed normally. For the present work, it was discovered that a linear relation was established between them, and they were adequately distributed along a straight line with negligible deviation. Figure 4.8 (c) shows a relationship between the residuals and RSM-based predicted values. The RSM software provided a graphical plot between predicted values (X-axis) and internally studentized residuals (Y-axis). According to the plot, no regular pattern was obtained; therefore, the developed model equation was adequate and validated the assumption of constant variance for the residuals [69]. Figure 4.8 (d) represents the relationship between the experimental run number and internally studentized residuals. A random distribution plot without any fixed pattern in the range of –3.00 to +3.00 proves the reliability and adequacy of the chosen model [69,70]. According to the modeling equation, ANOVA investigation, and various statistical parameters, it is concluded that the RSM-CCD with quadratic model clears all preliminary examinations.

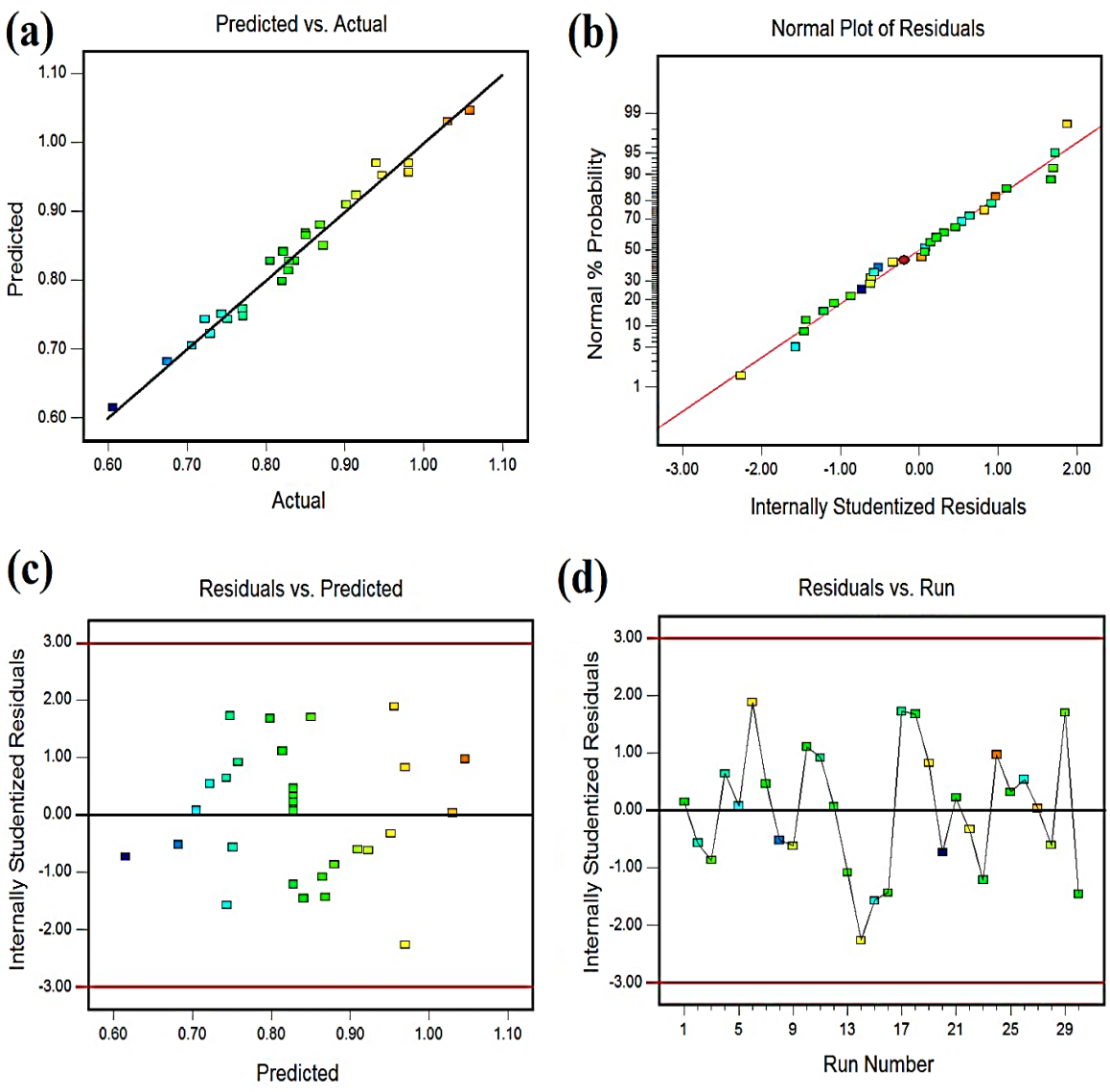

Figure 4.8 (a) The relationship between the actual vs. predicted values for the estimation of equilibrium CO_2 loading as a final response (Y) for the novel aqueous amine blend of HMDA+DMAE; (b) Normal plot of residuals establishing a relationship between the internally studentized residuals vs. normal % probability; (c) Relationship between the predicted values of the final response (Y) vs. internally studentized residuals; (d) Correlation between the run number vs. internally studentized residuals.

4.4.11.9 Analysis of 3-D surfaces and contour graphs

Analysis of 3-D surfaces and contour graphs signifies the most crucial part of the RSM software, and it is nothing but the graphical representation of independent variables and their effect on the final response [2,68,70,122,124]. Figure 4.9 (a) and (b) are the 3-D surface and contour graphs representing the factors and their effect on α value. Temperature (A) and CO_2 partial pressure (B) were the independent variables, and their influence on the response has been shown. It was evidenced that the equilibrium CO_2 loading decreased as the temperature enhanced. It was because of the well-known scenario that on increasing the temperature of the aqueous amine blend, the equilibrium shifts in the reverse direction, and simultaneously, the desorption of CO_2 gas also takes place, resulting in a lowering of α value. Similarly, when CO_2 partial pressure increased from 13.93 to 21.53 kPa, the equilibrium CO_2 loading also increased accordingly. It is well known that Henry's law governs the solubility of a gas in the liquid phase, and as the value of CO_2 partial pressure enhances, more CO_2 gas molecules are present in the system, which ultimately increases the gas solubility in the liquid. A detailed description of the effect of temperature and CO_2 partial pressure on α value has been incorporated in the previous sections of 4.4.1.1 and 4.4.1.2, respectively. Based on the above discussion, the collective effect of interaction among the factors 'A' and 'B' concluded that the equilibrium CO_2 loading would be maximum for low temperature and high CO_2 partial pressure. Figure 4.9 (c) and (d) represent the 3-D surface and contour graph for the factors, i.e., temperature (A) and mole fraction of HMDA (C), and their effect on the final response. It was discovered that on increasing the value of the mole fraction of HMDA in the aqueous amine blend of HMDA+DMAE from 0.09 to 0.16, the response also increased accordingly.

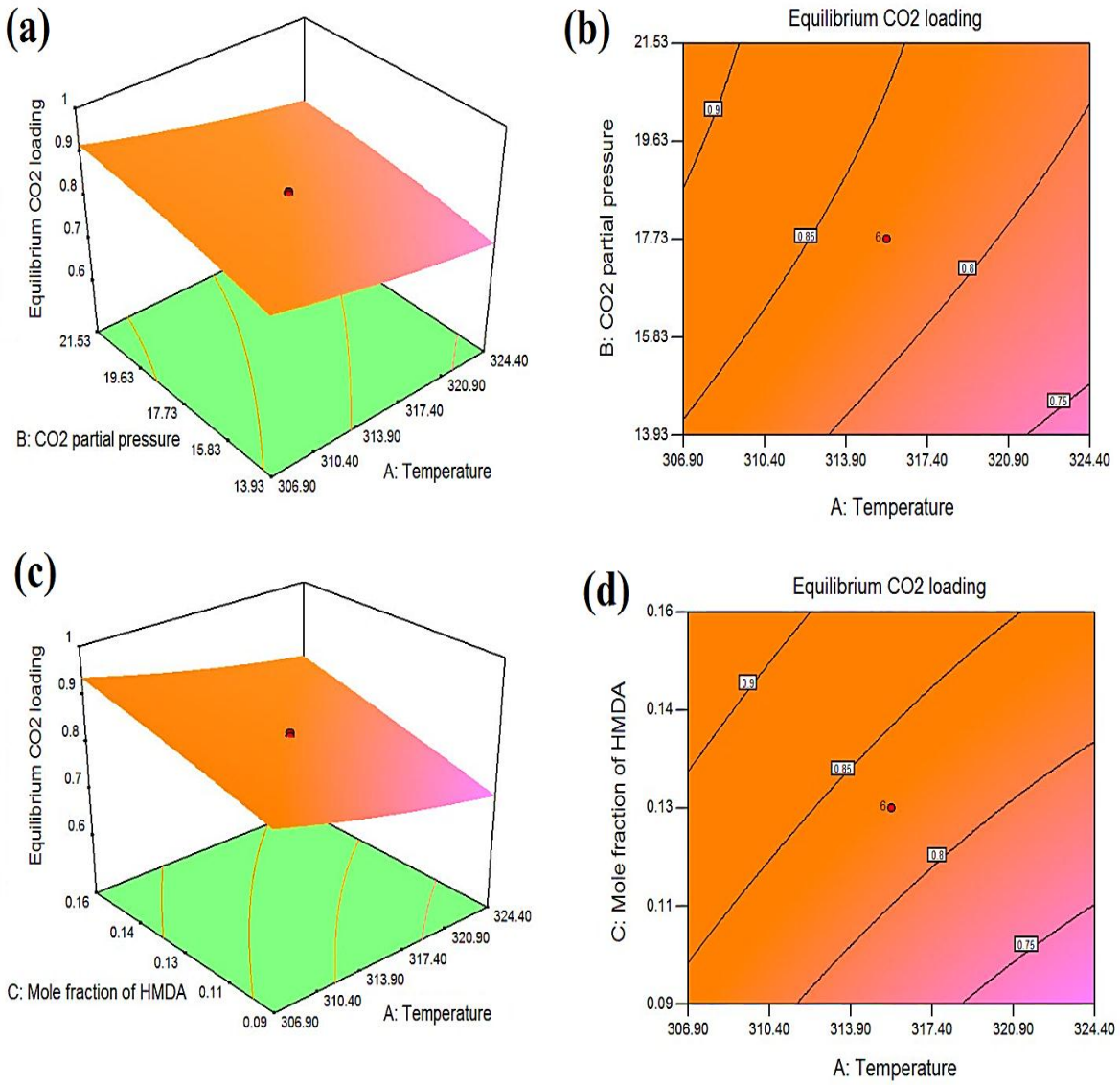

Figure 4.9 (a) 3-D surface representation of factors, i.e., temperature (A) and CO_2 partial pressure (B) and their effect on equilibrium CO_2 loading as a final response; (b) Contour graphical representation of factors, i.e., temperature (A) and CO_2 partial pressure (B) and their effect on equilibrium CO_2 loading as a final response; (c) 3-D surface representation of factors, i.e., temperature (A) and mole fraction of HMDA (C) and their effect on equilibrium CO_2 loading as a final response; (d) Contour graphical representation of factors, i.e., temperature (A) and mole fraction of HMDA (C) and their effect on equilibrium CO_2 loading as a final response.

The main reason for this scenario is that when the activator's mole fraction (i.e., HMDA) increases, the number of reactive sites also increases, causing a large amount of bicarbonate and carbonate ions formation, leading to an increase in the final response. A detailed description of the effect of increasing HMDA's mole fraction in the novel HMDA+DMAE amine blend on α value has already been discussed in the previous section of 4.4.1.3. Based on the above discussion, the collective interaction effect among the factors 'A' and 'C' suggested that the equilibrium CO_2 loading will be maximum for low temperature and high mole fraction of HMDA.

Figure 4.10 (a) and (b) represent the 3-D surface and contour graphs representing the factors and their effect on α value. Temperature (A) and solution concentration (D) were the factors that influenced the final response. It was found that on enhancing the value of solution concentration from 1.5 to 2.5 mol/L, the α value decreased. When the solution concentration increases, the steric hindrance of the solution also increases simultaneously. The steric hindrance becomes a barrier to the conversion of carbamate into bicarbonate in the gas-liquid reaction, which finally decreases the equilibrium CO_2 loading. A detailed description of the effect of increasing solution concentration on equilibrium CO_2 loading has already been discussed in section 4.4.1.4. Based on the above discussion, the collective interaction effect among the factors 'A' and 'D' informed that the equilibrium CO_2 loading would be maximum for low temperature and low solution concentration. Figure 4.10 (c) and (d) are the 3-D surface and contour representations of factors 'B' and 'C' and their effect on equilibrium CO_2 loading. The collective interaction effect among the factors 'B' and 'C' suggested that the maximum α value was at the maximum value of CO_2 partial pressure and mole fraction of HMDA.

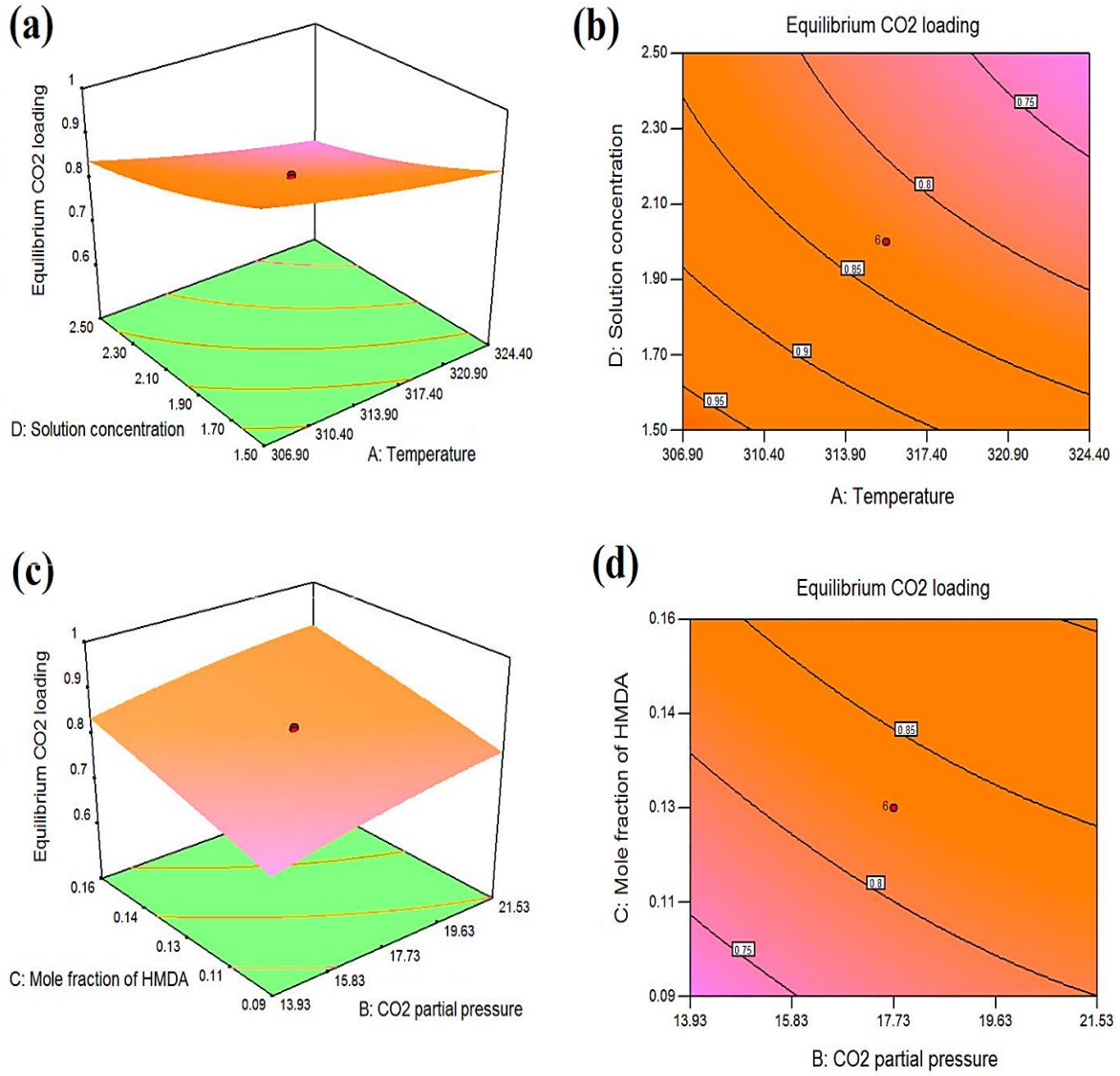

Figure 4.10 (a) 3-D surface representation of factors, i.e., temperature (A) and solution concentration (D) and their effect on equilibrium CO_2 loading as a final response; (b) Contour graphical representation of factors, i.e., temperature (A) and solution concentration (D) and their effect on equilibrium CO_2 loading as a final response; (c) 3-D surface representation of factors, i.e., CO_2 partial pressure (B) and mole fraction of HMDA (C) and their effect on equilibrium CO_2 loading as a final response; (d) Contour graphical representation of factors, i.e., CO_2 partial pressure (B) and mole fraction of HMDA (C) and their effect on equilibrium CO_2 loading as a final response.

Figure 4.11 (a) and (b) represent the 3-D surface and contour graph for the factors 'B' and 'D' and their effect on μ value as a final response. This graphical representation targeted the interaction of factors, i.e., P_{CO2} and C. It was encountered that the maximum α value was found at the highest value of P_{CO2} and lowest value of C. The effect of T, P_{CO2}, m_{HMDA} and C on α value has been discussed in detail in the previous sections. Therefore, in this chain, finally, Figure 4.11 (c) and (d) represent the interaction between the mole fraction of HMDA and solution concentration, and they were shown in terms of 3-D surfaces and contour graphs, respectively. The maximum mole fraction of HMDA and minimum solution concentration yielded the maximum equilibrium CO_2 loading.

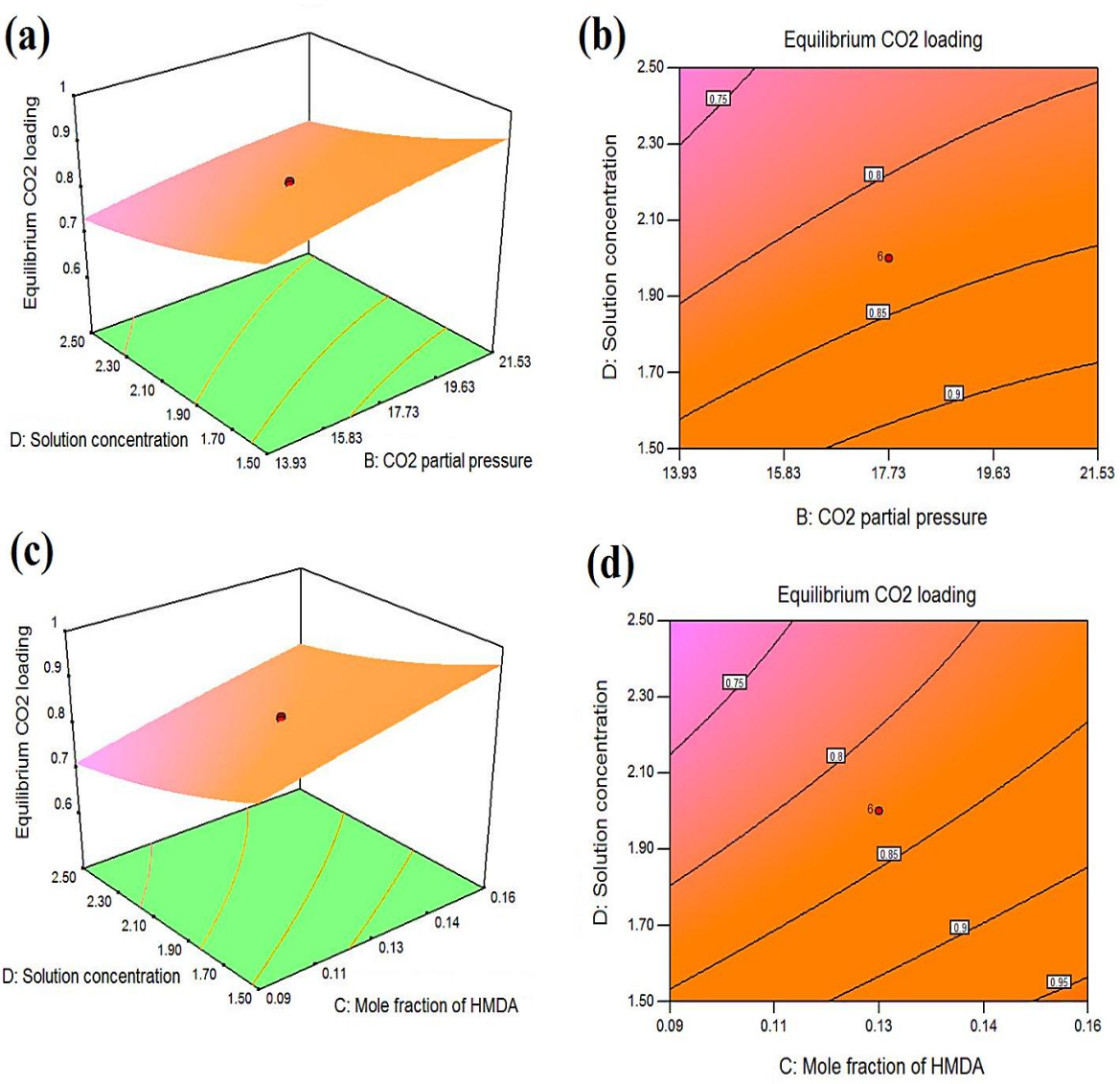

Figure 4.11 (a) 3-D surface representation of factors, i.e., CO_2 partial pressure (B) and solution concentration (D) and their effect on equilibrium CO_2 loading as a final response; (b) Contour graphical representation of factors, i.e., CO_2 partial pressure (B) and solution concentration (D) and their effect on equilibrium CO_2 loading as a final response; (c) 3-D surface representation of factors, i.e., mole fraction of HMDA (C) and solution concentration (D) and their effect on equilibrium CO_2 loading as a final response; (d) Contour graphical representation of factors, i.e., mole fraction of HMDA (C) and solution concentration (D) and their effect on equilibrium CO_2 loading as a final response.

4.4.11.10 Optimum value prediction and its validation by the RSM

After successfully examining the 3-D surfaces and contour graphs for the final response corresponding to various factors present in the system, the next step was to evaluate the optimum predicted value by the RSM software. For making predictions, initially, in the numerical optimization section, assigning the desired goals for different independent variables and the final response was mandatory. For factors like temperature (A), CO_2 partial pressure (B), mole fraction of HMDA (C), and solution concentration (D), 'in range' goal was set, but for equilibrium CO_2 loading, the maximum goal was chosen. Factor's lower and upper limits: A = 306.90–324.40 K, B = 13.93–21.53 kPa, C = 0.0875–0.1625, and D = 1.5–2.5 mol/L. The importance for independent variables present in the system was set as the default value of 3, but the response was to be maximized; therefore, its importance value was set to 5. Table 4.4 shows the required goals, lower and upper limits, and importance of independent variables along with its final response. The ramp data in the numerical solution section provided the desirability value for 45 different experimental sets generated by the software. The optimum value prediction was done to attain the final response, and the same is shown in Figure 4.12. At temperature (A) = 306.90 K, CO_2 partial pressure (B) = 21.53 kPa, mole fraction of HMDA (C) = 0.16, and solution concentration (D) = 1.5 mol/L, the RSM software yielded the optimum α value of 1.04583 mol CO_2/mol amine. The aforementioned operating condition was for the solution 1 out of 45 possibilities. The desirability lies in the range of 0 to 1, and a value closer to 1 always authenticates the system. The desirability of the current experimental work was found to be 0.972.

Table 4.4 Numerical solutions, goal, lower and upper limits of the individual constraints in order to calculate the overall desirability of the system.

Factors	Goal	Lower limit	Upper limit	Lower weight	Upper weight	Importance
A: Temperature	In range	306.90	324.40	1	1	3
B: CO_2 partial pressure	In range	13.93	21.53	1	1	3
C: Mole fraction of HMDA	In range	0.0875	0.1625	1	1	3
D: Solution concentration	In range	1.5	2.5	1	1	3
Equilibrium CO_2 loading	Maximize	0.6054	1.0586	1	1	5

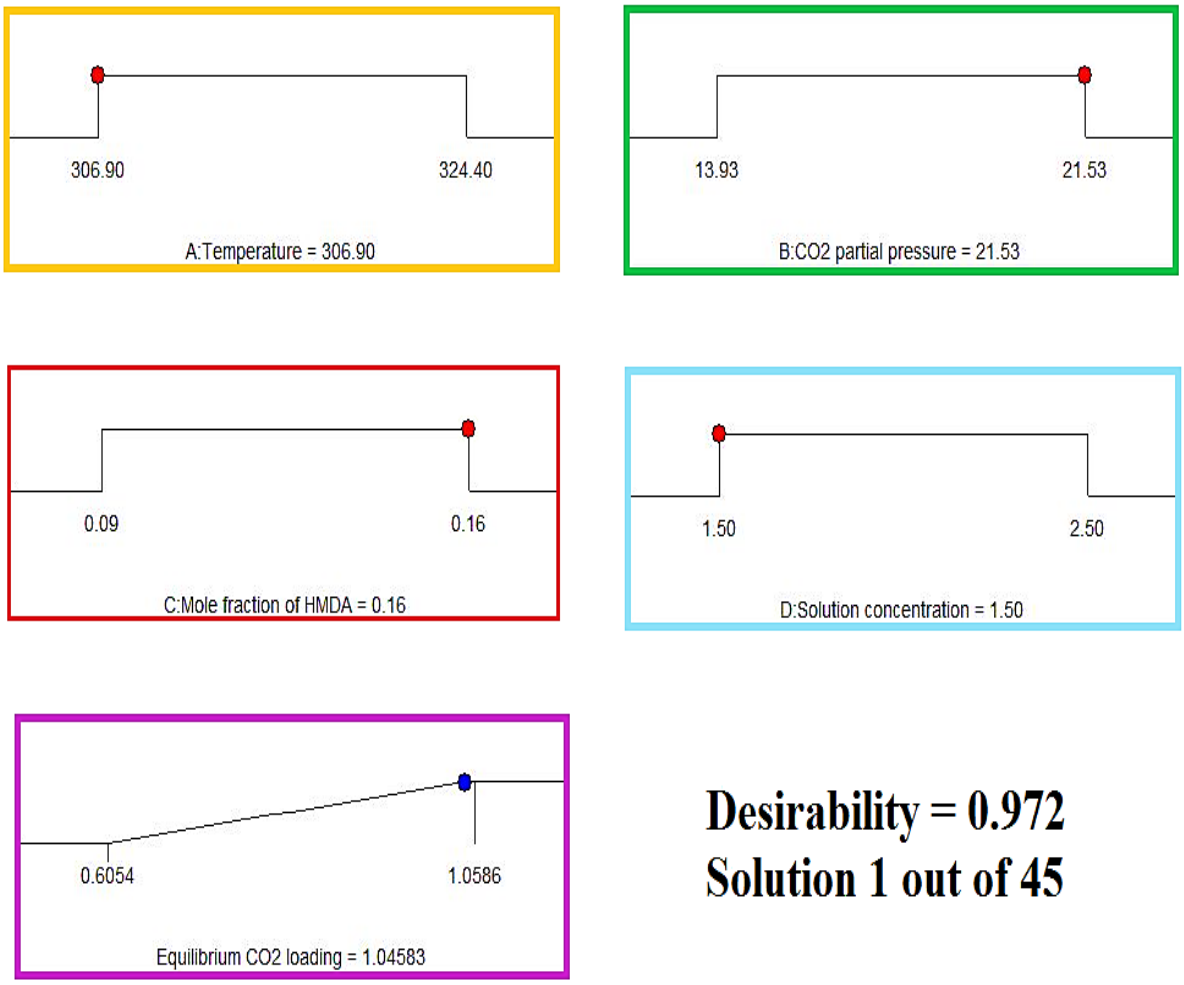

Figure 4.12 Desirability ramp for numerical optimization of independent variables and equilibrium CO_2 loading as a final response.

It was just the prediction by the software, but its authentication was required. To validate the prediction, two separate sets of experiments were conducted. Condition 1st: T = 306.90 K, P_{CO2} = 21.53 kPa, m_{HMDA} = 0.16, and C = 1.4 mol/L; Condition 2nd: T = 306.90 K, P_{CO2} = 21.53 kPa, m_{HMDA} = 0.16, and C = 1.6 mol/L. A minute variation in solution concentration for the novel HMDA+DMAE amine blend was done, and the experiments were conducted on the lab scale. Table 4.5 shows the RSM predicted and actual experimental results for estimating the optimum α value. The final response, i.e., μ value was estimated for both the operating conditions, i.e., condition 1st and condition 2nd. The predicted response was finally compared with two operating conditions. The α value for conditions 1st and condition 2nd was 1.05785 mol CO_2/mol amine and 1.02568 mol CO_2/mol amine, respectively. The average value of the final response for both operating conditions was determined to be 1.04176 mol CO_2/mol amine. This average value is much closer to the value predicted by the RSM software, and it was less than 1 % of the predicted value. Therefore, it can be inferred from the entire investigation that the experimental results validated the optimum predictions made by the RSM software.

Table 4.5 RSM predicted optimized result vs. actual experimental results.

	Temperature (K)	**CO_2 partial pressure (kPa)**	**Mole fraction of HMDA**	**Solution concentration (mol/L)**	**Final response, Y (mol CO_2/mol amine)**
Experimental value	306.90	21.53	0.16	1.40	1.05785
Predicted value	306.90	21.53	0.16	1.50	1.04583
Experimental value	306.90	21.53	0.16	1.60	1.02568

4.4.12 Toxicity assessment for the novel amine blend

The amine losses from the industrial unit due to technical issues form the degradation products that react in the environment and mix in soil, rivers, ponds, lakes, oceans, and other water bodies in the form of rain [95]. The toxicity of the novel HMDA+DMAE amine blend was judged by acquiring the data of LD_{50} value from the MSDS. The toxicity assessment targeted LD_{50} values of HMDA and DMAE along with other conventional amines used in post-combustion CO_2 capture. These traditional amines were MDEA, AMP, DMAE, PZ, DEA, DEEA, HMDA, MEA, 2-(Butylamino)ethanol (BAE), and 3-Dimethylamino-1-propanol (3DMAP). The chemical consumption by rats, which causes 50 % fatality amongst the rats (LD_{50}), was considered during the entire toxicity assessment. For the chosen traditional amines, the LD_{50} values ranged from 442–4680 mg/Kg. The highest and lowest values of LD_{50} among the selected amines were discovered to be 4680 mg/Kg and 442 mg/Kg, corresponding to MDEA [125] and 3DMAP [126], respectively. It is well known that a higher value of LD_{50} signifies that the amine is less toxic, and a lower value represents the high toxicity of the amine. Various traditional amines, along with HMDA and DMAE with different LD_{50} values are shown in Figure 4.13.

According to the MSDS, the traditional MEA [127] has an LD_{50} value of 1089 mg/kg, which places it in the third category according to the EPA and is slightly toxic. The LD_{50} values of DMAE [128] and HMDA [129] were found to be 2000 mg/Kg and 1160 mg/Kg, respectively. These values are higher than MEA, meaning they are less toxic than MEA. Information based on the toxicity of amine, as provided in the B8 of Appendix – B, none of the investigated amines have been classified under the first and fourth categories of toxicity, according to the classification provided by EPA. It signifies that neither of them is

highly toxic nor safe to use. Amongst all these amines, only 3DMAP showed moderately toxic behavior with an LD_{50} value of 442 mg/Kg. Likewise, AMP [130], PZ [131], DEA [132], DEEA [133], and BAE [134] have shown toxicity of 2900 mg/Kg, 1900 mg/Kg, 1300 mg/Kg, and 890 mg/Kg, respectively. It was discovered that the toxicity of DMAE and HMDA was lower than that of conventional MEA with slight toxic behavior, which is a commendable factor from an environmental and human health point of view. Therefore, HMDA and DMAE can be adopted to prepare the novel aqueous amine blend of HMDA+DMAE for post-combustion CO_2 capture.

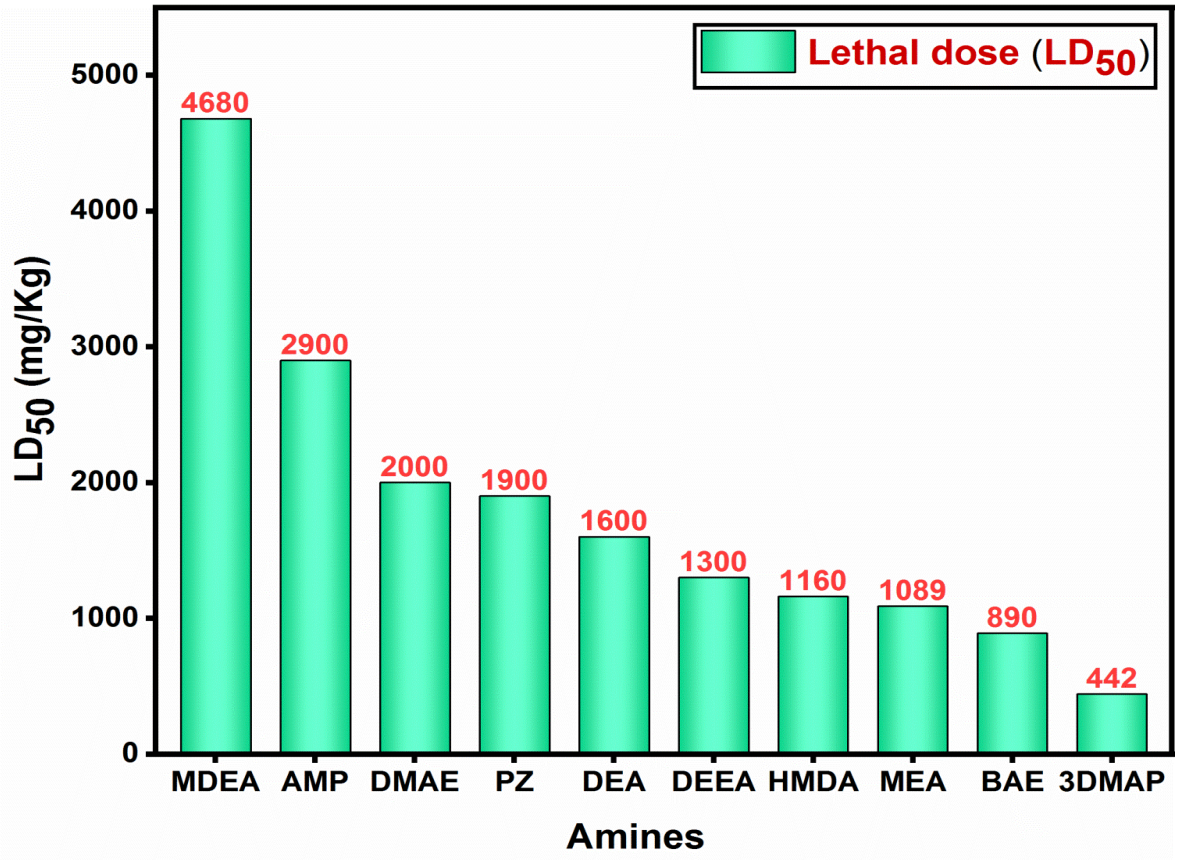

Figure 4.13 Toxicity assessment in terms of LD_{50} values for various conventional amines.

4.5 Conclusions

In the present experimental work, a potential novel aqueous HMDA+DMAE amine blend was prepared, which demonstrated its outstanding performance in contributing towards net-zero CO_2 emissions. The performance of this novel blend was examined by conducting a CO_2 absorption and desorption investigation. The experimental investigation has targeted equilibrium CO_2 loading, absorption capacity, cyclic equilibrium CO_2 loading, cyclic capacity, pH, density, ^{13}C NMR and FTIR spectroscopic analysis, heat duty and regeneration efficiency, CO_2 absorption and desorption rate, heat of CO_2 absorption, RSM modeling and optimization, and toxicity assessment. Initially, the CO_2-absorption experimental setup was validated, and the experiments were conducted on the operating conditions as: T = 298.15–333.15 K, P_{CO2} = 10.13–25.33 kPa, m_{HMDA} = 0.05–0.20, and C = 1–3 mol/L. The effect of T, P_{CO2}, m_{HMDA}, C, and operating time on α value revealed that on increasing the T and C, the α value decreased, while on increasing P_{CO2} and m_{HMDA}, the α value increased. Likewise, as operating time increases, the α value increases up to a certain time, and then it becomes sluggish. It was determined that the maximum equilibrium CO_2 loading (α_{max}) of 1.2174 mol CO_2/mol amine was attained at T = 298.15 K, P_{CO2} = 25.33 kPa, m_{HMDA} = 0.20, and C = 1 mol/L. The developed semi-empirical model validated 40 experimental run sets in the absorption investigation, which yielded a fabulous % AARD of 3.06 %, which was highly reliable and accurate. pH for CO_2-unloaded, CO_2-loaded, and CO_2-regenerated aqueous amine blend samples fall in the range of 12.04–12.78, 8.37–9.50, and 9–11, respectively. The solution concentration significantly affected the solution pH, and it slightly increased while increasing the solution concentration. Similarly, density depended on the solution concentration and was almost

similar for every CO_2-unloaded samples. The density increased with CO_2 loading and decreased on regenerating the CO_2-loaded samples. Run no. 09: α_{max} = 1.2174 mol CO_2/mol amine, $\rho_{unloaded}$ = 995.7 kg/m^3, ρ_{loaded} = 1035.6 kg/m^3, and $\rho_{regenerated}$ = 1011.4 kg/m^3; Run no. 40: α_{min} = 0.7155 mol CO_2/mol amine, $\rho_{unloaded}$ = 986.1 kg/m^3, ρ_{loaded} = 1058.8 kg/m^3, and $\rho_{regenerated}$ = 1018.9 kg/m^3. ^{13}C NMR and FTIR investigation were used to characterize the CO_2-unloaded, CO_2-loaded, and CO_2-regenerated amine blend samples. The characterization methods authenticated the chemical reactions and provided information about the intermediate complexes formed. The CO_2-loaded samples were regenerated, and heat duty for C = 1, 2, and 3 mol/L was found to be 357.11, 164.18, and 131.24 kJ/mol CO_2, which was 20.64 %, 63.51 %, and 70.83 % less than the 30 wt% MEA, respectively. It was also found that on enhancing the molar ratio of HMDA in the HMDA+DMAE amine blend, the value of heat duty of regeneration also increased accordingly. The regeneration efficiency for the novel HMDA+DMAE amine blend for run no. 07, 21, 34, and 30 wt% MEA was found to be 52.21 %, 63.51 %, 60.47 %, and 31.23 %, respectively. In this series, the trend of initial absorption rate at T = 313.15 K, P_{CO2} = 25.33 kPa, and C = 3 mol/L: 0.5 mol/L HMDA–2.5 mol/L DMAE < 1 mol/L HMDA–2 mol/L DMAE < 1.5 mol/L HMDA–1.5 mol/L DMAE < 2 mol/L HMDA–1 mol/L DMAE. The initial CO_2 absorption rate of 2 mol/L HMDA–1 mol/L DMAE was 26 × 10^{-4} mol CO_2/(L solution. min), yielded a 62.5% higher absorption rate than 30 wt% MEA. The initial CO_2-desorption rate follows the inverse relation as compared with the initial CO_2-absorption rate, therefore; the initial CO_2-desorption rate for 0.5 mol/L HMDA–2.5 mol/L DMAE was 43.75 % higher than the benchmark 30 wt% MEA. The heat of CO_2 absorption for the novel HMDA+DMAE amine blend was calculated to be –75.50 kJ/mol CO_2, which

was less than the conventional 30 wt% MEA. RSM predicted α_{max} of 1.04583 mol CO_2/mol amine attained at T = 306.90 K, P_{CO2} = 21.53 kPa, m_{HMDA} = 0.16, and C = 1.5 mol/L. The toxicity of DMAE (LD_{50} = 2000 mg/kg) and HMDA (LD_{50} = 1160 mg/kg) was lower than traditional MEA with slight toxic behavior, which is a commendable aspect from an environmental and human health point of view. Based on the commendable performance, the novel HMDA+DMAE blend is highly recommended for industrial applications.

ASSOCIATED CONTENT

Appendix – A and Appendix – B

Figure A7 to Figure A9, related to this chapter, can be found in Appendix–A.

Table B5, Table B6, Table B9, and Table B11 to Table B14, and content B7, B8, and B10 related to this chapter, can be found in Appendix-B.

References

[1] Gautam A, Mondal MK. Post-combustion capture of CO_2 using novel aqueous triethylenetetramine and 2-dimethylaminoethanol amine blend: equilibrium CO_2 loading-empirical model and optimization, CO_2 desorption, absorption heat, and ^{13}C NMR analysis. Fuel. 2023;331:125864. https://doi.org/10.1016/j.fuel.2022.125864

[2] Gautam A, Mondal MK. Novel aqueous amine blend of 2-(Butylamino) ethanol and 2-Dimethylaminoethanol for CO_2 capture: Equilibrium CO_2 loading, RSM optimization, desorption study, characterization and toxicity assessment. Sep Purif Technol. 2023;322:124279. https://doi.org/10.1016/j.seppur.2023.124279

[3] Gautam A, Mondal MK. Review of recent trends and various techniques for CO_2 capture: Special emphasis on biphasic amine solvents. Fuel. 2023;334:126616. https://doi.org/10.1016/j.fuel.2022.126616

[4] Zhang R, Li Y, He X, Niu Y, Li CE, Amer MW, Barzagli F. Investigation of the improvement of the CO_2 capture performance of aqueous amine sorbents by switching from dual-amine to trio-amine systems. Sep Purif Technol. 2023;316:123810. https://doi.org/10.1016/j.seppur.2023.123810

[5] Agnihotri N, Gupta GK, Mondal MK. Thermo-kinetic analysis, thermodynamic parameters and comprehensive pyrolysis index of Melia azedarach sawdust as a genesis of bioenergy. Biomass Conv Bioref 2022;1-8. https://doi.org/10.1007/s13399-022-02524-y

[6] He X, He H, Barzagli F, Amer MW, Li CE, Zhang R. Analysis of the energy consumption in solvent regeneration processes using binary amine blends for CO_2 capture. Energy. 2023;270:126903. https://doi.org/10.1016/j.energy.2023.126903

[7] Zhao S, Wang Y, Zhu K, Zhao D, Song Q. Improving the absorption load, high viscosity, and regeneration efficiency of CO_2 capture using a novel tri-solvent biphasic solvents of TETA-AMP-1DMA2P. Environ Sci Pollut Res 2022;29:84903-15. https://doi.org/10.1007/s11356-022-21822-6

[8] Pandey D, Mondal MK. Thermodynamic modeling and new experimental CO_2 solubility into aqueous EAE and AEEA blend, heat of absorption, cyclic absorption capacity and desorption study for post-combustion CO_2 capture. Chem Eng J. 2021;410:128334. https://doi.org/10.1016/j.cej.2020.128334

[9] Pandey D, Mondal MK. Equilibrium CO_2 solubility in the aqueous mixture of MAE and AEEA: Experimental study and development of modified thermodynamic model. Fluid Ph Equilibria. 2020;522:112766. https://doi.org/10.1016/j.fluid.2020.112766

[10] Gupta AK, Gautam A, Mondal MK. Experimental, modeling and RSM optimization of CO_2 loading for an aqueous blend of diethylenetriamine and 3-dimethyl amino-1-propanol. Korean J Chem Eng 2023;40:1151-67. https://doi.org/10.1007/s11814-022-1300-3

[11] Lv B, Guo B, Zhou Z, Jing G. Mechanisms of CO_2 capture into monoethanolamine solution with different CO_2 loading during the absorption/desorption processes. Environ Sci Technol 2015;49:10728-35. https://doi.org/10.1021/acs.est.5b02356

[12] Mazari SA, Kang TH, Devkota S, Cha JY, Shin BJ, Mun JH, Kim KM, Lee U, Moon JH. Investigating the effect of blending of diamine and alkanolamine for CO_2 capture: Experiment and thermodynamic modeling of CO_2-AEEA-DEA-H_2O system. Chem Eng J. 2023;470:144141. https://doi.org/10.1016/j.cej.2023.144141

[13] Kumari M, Vega F, Fernández LM, Shadangi KP, Kumar N. Liquid Amine functional, aqueous blends and the CO_2 absorption capacity: molecular structure, size, interaction

parameter and mechanistic aspects. J Mol Liq. 2023;384:122288. https://doi.org/10.1016/j.molliq.2023.122288

[14] Perumal M, Jayaraman D, Balraj A. Experimental studies on CO_2 absorption and solvent recovery in aqueous blends of monoethanolamine and tetrabutylammonium hydroxide. Chemosphere. 2021;276:130159. https://doi.org/10.1016/j.chemosphere.2021.130159

[15] Kumar S, Mondal MK. Selection of efficient absorbent for CO_2 capture from gases containing low CO_2. Korean J Chem Eng 2020;37:231-9. https://doi.org/10.1007/s11814-019-0440-6

[16] Kim J, Lee J, Lee Y, Kim H, Kim E, Lee KS. Evaluation of aqueous polyamines as CO_2 capture solvents. Energy. 2019;187:115908. https://doi.org/10.1016/j.energy.2019.115908

[17] Ji L, Yu H, Li K, Yu B, Grigore M, Yang Q, Wang X, Chen Z, Zeng M, Zhao S. Integrated absorption-mineralisation for low-energy CO_2 capture and sequestration. Appl Energy 2018;225: 356-66. https://doi.org/10.1016/j.apenergy.2018.04.108

[18] Bains P, Psarras P, Wilcox J. CO_2 capture from the industry sector. Prog Energy Combust Sci 2017;63:146-72. https://doi.org/10.1016/j.pecs.2017.07.001

[19] Gao G, Jiang W, Li X, Zhao Z, Jiang C, Luo C, Wu F, Zhang L. Novel assessment of highly efficient polyamines for post-combustion CO_2 capture: Absorption heat, reaction rate, CO_2 cyclic capacity, and phase change behavior. Sep Purif Technol. 2023;306:122615. https://doi.org/10.1016/j.seppur.2022.122615

[20] Li T, Yang C, Tantikhajorngosol P, Sema T, Shi H, Tontiwachwuthikul P. Experimental investigations and the modeling approach for CO_2 solubility in aqueous

blended amine systems of monoethanolamine, 2-amino-2-methyl-1-propanol, and 2-(butylamino) ethanol. Environ Sci Pollut Res 2022;29:69402-23. https://doi.org/10.1007/s11356-022-20411-x

[21] Shen Y, Jiang C, Zhang S, Chen J, Wang L, Chen J. Biphasic solvent for CO_2 capture: Amine property-performance and heat duty relationship. Appl Energy 2018;230:726-33. https://doi.org/10.1016/j.apenergy.2018.09.005

[22] Zhang S, Shen Y, Shao P, Chen J, Wang L. Kinetics, thermodynamics, and mechanism of a novel biphasic solvent for CO_2 capture from flue gas. Environ Sci Technol 2018;52:3660-8. https://doi.org/10.1021/acs.est.7b05936

[23] Sreedhar I, Nahar T, Venugopal A, Srinivas B. Carbon capture by absorption–Path covered and ahead. Renew Sustain Energy Rev 2017;76:1080-107. https://doi.org/10.1016/j.rser.2017.03.109

[24] Muchan P, Saiwan C, Narku-Tetteh J, Idem R, Supap T, Tontiwachwuthikul P. Screening tests of aqueous alkanolamine solutions based on primary, secondary, and tertiary structure for blended aqueous amine solution selection in post combustion CO_2 capture. Chem Eng Sci 2017;170:574-82. https://doi.org/10.1016/j.ces.2017.02.031

[25] Ping T, Dong Y, Shen S. Densities, viscosities and spectroscopic study of partially CO_2-loaded nonaqueous blends of 2-butoxyethanol with 2-(ethylamino) ethanol and 2-(butylamino) ethanol at temperatures of (293.15 to 353.15) K. J Mol Liq. 2020;312:113389. https://doi.org/10.1016/j.molliq.2020.113389

[26] Arshad N, Alhajaj A. Process synthesis for amine-based CO_2 capture from combined cycle gas turbine power plant. Energy. 2023;274:127391. https://doi.org/10.1016/j.energy.2023.127391

[27] Singh S, Pandey D, Mondal MK. New experimental data on equilibrium CO_2 loading into aqueous 3-dimethyl amino-1-propanol and 1, 5-diamino-2-methylpentane blend: Empirical model and CO_2 absorption enthalpy. J Chem Eng Data 2020;66:740-8. https://doi.org/10.1021/acs.jced.0c00851

[28] Hafizi A, Mokari MH, Khalifeh R, Farsi M, Rahimpour MR. Improving the CO_2 solubility in aqueous mixture of MDEA and different polyamine promoters: The effects of primary and secondary functional groups. J Mol Liq. 2020;297:111803. https://doi.org/10.1016/j.molliq.2019.111803

[29] Kim YE, Yun SH, Choi JH, Nam SC, Park SY, Jeong SK, Yoon YI. Comparison of the CO_2 absorption characteristics of aqueous solutions of diamines: absorption capacity, specific heat capacity, and heat of absorption. Energy Fuels 2015;29:2582-90. https://doi.org/10.1021/ef500561a

[30] Yang C, Li T, Tantikhajorngosol P, Sema T, Xiao M, Tontiwachwuthikul P. Evaluation of novel aqueous piperazine-based physical-chemical solutions as biphasic solvents for CO_2 capture: Initial absorption rate, equilibrium solubility, phase separation and desorption rate. Chem Eng Sci. 2023;277:118852. https://doi.org/10.1016/j.ces.2023.118852

[31] Wai SK, Nwaoha C, Saiwan C, Idem R, Supap T. Absorption heat, solubility, absorption and desorption rates, cyclic capacity, heat duty, and absorption kinetic modeling of AMP–DETA blend for post–combustion CO_2 capture. Sep Purif Technol 2018;194:89-95. https://doi.org/10.1016/j.seppur.2017.11.024

[32] Arshad MW, Von Solms N, Thomsen K. Thermodynamic modeling of liquid–liquid phase change solvents for CO_2 capture. Int J Greenh Gas Control 2016;53:401-24. https://doi.org/10.1016/j.ijggc.2016.08.014

[33] Shi H, Naami A, Idem R, Tontiwachwuthikul P. Catalytic and non catalytic solvent regeneration during absorption-based CO_2 capture with single and blended reactive amine solvents. Int J Greenh Gas Control 2014;26:39-50. https://doi.org/10.1016/j.ijggc.2014.04.007

[34] Mun JH, Shin BJ, Kim SM, You JK, Park YC, Chun DH, Lee JS, Min BM, Lee U, Kim KM, Moon JH. Optimal MEA/DIPA/water blending ratio for minimizing regeneration energy in absorption-based carbon capture process: Experimental CO_2 solubility and thermodynamic modeling. Chem Eng J. 2022;444:136523. https://doi.org/10.1016/j.cej.2022.136523

[35] Choi BK, Kim SM, Lee JS, Park YC, Chun DH, Shin HY, Sung HJ, Min BM, Moon JH. Effect of blending ratio and temperature on CO_2 solubility in blended aqueous solution of monoethanolamine and 2-amino-2-methyl-propanol: experimental and modeling study using the electrolyte nonrandom two-liquid model. ACS omega 2020;5:28738-48. https://doi.org/10.1021/acsomega.0c04046

[36] Ping T, Dong Y, Shen S. Energy-efficient CO_2 capture using nonaqueous absorbents of secondary alkanolamines with a 2-butoxyethanol cosolvent. ACS Sustain Chem Eng 2020;8: 18071-82. https://doi.org/10.1021/acssuschemeng.0c06345

[37] Mondal BK, Bandyopadhyay SS, Samanta AN. Kinetics of CO_2 absorption in aqueous hexamethylenediamine. Int J Greenh Gas Control 2017;56:116-25. https://doi.org/10.1016/j.ijggc.2016.11.023

[38] Vaidya PD, Kenig EY. CO_2-alkanolamine reaction kinetics: a review of recent studies. Chem Eng Technol 2007;30:1467-74. https://doi.org/10.1002/ceat.200700268

[39] Hu X, Huang J, He X, Luo Q, Li CE, Zhou C, Zhang R. Analyzing the potential benefits of trio-amine systems for enhancing the CO_2 desorption processes. Fuel. 2022;316:123216. https://doi.org/10.1016/j.fuel.2022.123216

[40] Chen M, Li M, Zhang F, Hu X, Wu Y. Fast and efficient CO_2 absorption in non-aqueous tertiary amines promoted by ethylene glycol. Energy Fuels 2022;36:4830-6. https://doi.org/10.1021/acs.energyfuels.2c00215

[41] Kim YE, Moon SJ, Yoon YI, Jeong SK, Park KT, Bae ST, Nam SC. Heat of absorption and absorption capacity of CO_2 in aqueous solutions of amine containing multiple amino groups. Sep Purif Technol 2014;122:112-8. https://doi.org/10.1016/j.seppur.2013.10.030

[42] Sanz-Pérez ES, Arencibia A, Sanz R, Calleja G. New developments on carbon dioxide capture using amine-impregnated silicas. Adsorption 2016;22:609-19. https://doi.org/10.1007/s10450-015-9740-2

[43] Xiao M, Liu H, Gao H, Liang Z. CO_2 absorption with aqueous tertiary amine solutions: Equilibrium solubility and thermodynamic modeling. J Chem Thermodyn 2018;122:170-82. https://doi.org/10.1016/j.jct.2018.03.020

[44] Narku-Tetteh J, Muchan P, Saiwan C, Supap T, Idem R. Selection of components for formulation of amine blends for post combustion CO_2 capture based on the side chain structure of primary, secondary and tertiary amines. Chem Eng Sci 2017;170:542-60. https://doi.org/10.1016/j.ces.2017.02.036

[45] Cao F, Gao H, Xiong Q, Liang Z. Experimental studies on mass transfer performance for CO_2 absorption into aqueous N, N-dimethylethanolamine (DMEA) based solutions in a PTFE hollow fiber membrane contactor. Int J Greenh Gas Control 2019;82:210-7. https://doi.org/10.1016/j.ijggc.2018.12.011

[46] El Hadri N, Quang DV, Goetheer EL, Zahra MR. Aqueous amine solution characterization for post-combustion CO_2 capture process. Appl Energy 2017;185:1433-49. https://doi.org/10.1016/j.apenergy.2016.03.043

[47] Mondal BK, Bandyopadhyay SS, Samanta AN. Vapor–liquid equilibrium measurement and ENRTL modeling of CO_2 absorption in aqueous hexamethylenediamine. Fluid Ph Equilibria 2015;402:102-12. https://doi.org/10.1016/j.fluid.2015.05.033

[48] Singh P, van Swaaij WP, Brilman DW. Kinetics study of carbon dioxide absorption in aqueous solutions of 1, 6-hexamethyldiamine (HMDA) and 1, 6-hexamethyldiamine, N, N′ di-methyl (HMDA, N, N′). Chem Eng Sci 2011;66:4521-32. https://doi.org/10.1016/j.ces.2011.06.008

[49] Pasha M, Li G, Shang M, Liu S, Su Y. Mass transfer and kinetic characteristics for CO_2 absorption in microstructured reactors using an aqueous mixed amine. Sep Purif Technol. 2021;274:118987. https://doi.org/10.1016/j.seppur.2021.118987

[50] Patil MP, Vaidya PD. Kinetics of CO_2 absorption into aqueous AMP/HMDA/TEG mixtures. ChemistrySelect 2018;3:195-200. https://doi.org/10.1002/slct.201702464

[51] Azhgan M, Farsi M, Eslamloueyan R. Solubility of CO_2 in aqueous solutions of DAMP+MDEA, DAMP+MEA, DAH+MDEA and DAH+MEA. J Nat Gas Sci Eng 2017;46: 526-32. https://doi.org/10.1016/j.jngse.2017.08.014

[52] El Hadri N, Quang DV, Goetheer EL, Zahra MR. Aqueous amine solution characterization for post-combustion CO_2 capture process. Appl Energy 2017;185:1433-49. https://doi.org/10.1016/j.apenergy.2016.03.043

[53] Ling H, Gao H, Liang Z. Comprehensive solubility of N_2O and mass transfer studies on an effective reactive N, N-dimethylethanolamine (DMEA) solvent for post-combustion CO_2 capture. Chem Eng J 2019;355:369-79. https://doi.org/10.1016/j.cej.2018.08.147

[54] Mokhtari Z, Pakravesh A, Zarei H. High-pressure densities of 2-(dimethylamino) ethanol and 2-(diethylamino) ethanol: Measurement and modeling with new modified Tait and PC-SAFT equations of state. Fluid Ph Equilibria. 2023;572:113825. https://doi.org/10.1016/j.fluid.2023.113825

[55] Sharif M, Zhang T, Wu X, Yu Y, Zhang Z. Evaluation of CO_2 absorption performance by molecular dynamic simulation for mixed secondary and tertiary amines. Int J Greenh Gas Control. 2020;97:103059. https://doi.org/10.1016/j.ijggc.2020.103059

[56] Sharif M, Fan H, Wu X, Yu Y, Zhang T, Zhang Z. Assessment of novel solvent system for CO_2 capture applications. Fuel. 2023;337:127218. https://doi.org/10.1016/j.fuel.2022.127218

[57] Zhang P, Xu R, Li H, Gao H, Liang Z. Mass transfer performance for CO_2 absorption into aqueous blended DMEA/MEA solution with optimized molar ratio in a hollow fiber membrane contactor. Sep Purif Technol 2019;211:628-36. https://doi.org/10.1016/j.seppur.2018.10.034

[58] Ling H, Liu S, Wang T, Gao H, Liang Z. Characterization and correlations of CO_2 absorption performance into aqueous amine blended solution of monoethanolamine (MEA)

and N, N-dimethylethanolamine (DMEA) in a packed column. Energy Fuels 2019;33:7614-25. https://doi.org/10.1021/acs.energyfuels.9b01764

[59] Jiang W, Luo X, Gao H, Liang Z, Liu B, Tontiwachwuthikul P, Hu X. A comparative kinetics study of CO_2 absorption into aqueous DEEA/MEA and DMEA/MEA blended solutions. AIChE J 2018;64:1350-8. https://doi.org/10.1002/aic.16024

[60] Chowdhury FA, Okabe H, Shimizu S, Onoda M, Fujioka Y. Development of novel tertiary amine absorbents for CO_2 capture. Energy Procedia 2009;1:1241-8. https://doi.org/10.1016/j.egypro.2009.01.163

[61] Buvik V, Vevelstad SJ, Brakstad OG, Knuutila HK. Stability of structurally varied aqueous amines for CO_2 capture. Ind Eng Chem Res 2021;60:5627-38. https://doi.org/10.1021/acs.iecr.1c00502

[62] Brúder P, Lauritsen KG, Mejdell T, Svendsen HF. CO_2 capture into aqueous solutions of 3-methylaminopropylamine activated dimethyl-monoethanolamine. Chem Eng Sci 2012;75:28-37. https://doi.org/10.1016/j.ces.2012.03.005

[63] Agnihotri N, Mondal MK. Process parameter variation of Melia azedarach sawdust pyrolysis for fuel properties, physicochemical characterization, and in-depth speciation analysis. Biomass Conv Bioref 2023:1-5. https://doi.org/10.1007/s13399-023-04305-7

[64] Zheng W, Yan Z, Zhang R, Jiang W, Luo X, Liang Z, Yang Q, Yu H. A study of kinetics, equilibrium solubility, speciation and thermodynamics of CO_2 absorption into benzylamine (BZA) solution. Chem Eng Sci. 2022;251:117452. https://doi.org/10.1016/j.ces.2022.117452

[65] Huang Q, Jing G, Zhou X, Lv B, Zhou Z. A novel biphasic solvent of amino-functionalized ionic liquid for CO_2 capture: High efficiency and regenerability. J CO_2 Util 2018;25:22-30. https://doi.org/10.1016/j.jcou.2018.03.001

[66] Zhou X, Liu F, Lv B, Zhou Z, Jing G. Evaluation of the novel biphasic solvents for CO_2 capture: Performance and mechanism. Int J Greenh Gas Control 2017;60:120-8. https://doi.org/10.1016/j.ijggc.2017.03.013

[67] Perinu C, Arstad B, Jens KJ. NMR spectroscopy applied to amine–CO_2–H_2O systems relevant for post-combustion CO_2 capture: A review. Int J Greenh Gas Control 2014;20:230-43. https://doi.org/10.1016/j.ijggc.2013.10.029

[68] Shafaghat J, Ghaemi A. Comparison of Pb (II) adsorption by ground granulated blast-furnace and phosphorus slags; exploitation of RSM. Iran J Sci Technol Trans Sci 2021;45:899-911. https://doi.org/10.1007/s40995-021-01075-7

[69] Asgarifard P, Rahimi M, Tafreshi N. Response surface modelling of CO_2 capture by ammonia aqueous solution in a microchannel. Can J Chem Eng 2021;99:601-12. https://doi.org/10.1002/cjce.23881

[70] Pashaei H, Ghaemi A, Nasiri M, Karami B. Experimental modeling and optimization of CO_2 absorption into piperazine solutions using RSM-CCD methodology. ACS Omega 2020;5:8432-48. https://doi.org/10.1021/acsomega.9b03363

[71] Shafeeyan MS, Daud WM, Houshmand A, Arami-Niya A. The application of response surface methodology to optimize the amination of activated carbon for the preparation of carbon dioxide adsorbents. Fuel 2012;94:465-72. https://doi.org/10.1016/j.fuel.2011.11.035

[72] Sibuh BZ, Gupta PK, Taneja P, Khanna S, Sarkar P, Pachisia S, Khan AA, Jha NK, Dua K, Singh SK, Pandey S. Synthesis, in silico study, and anti-cancer activity of

thiosemicarbazone derivatives. Biomedicines. 2021;9:1375. https://doi.org/10.3390/biomedicines9101375

[73] Gadaleta D, Vuković K, Toma C, Lavado GJ, Karmaus AL, Mansouri K, Kleinstreuer NC, Benfenati E, Roncaglioni A. SAR and QSAR modeling of a large collection of LD_{50} rat acute oral toxicity data. J Cheminformatics 2019;11:1-6. https://doi.org/10.1186/s13321-019-0383-2

[74] Strickland J, Clippinger AJ, Brown J, Allen D, Jacobs A, Matheson J, Lowit A, Reinke EN, Johnson MS, Quinn Jr MJ, Mattie D. Status of acute systemic toxicity testing requirements and data uses by US regulatory agencies. Regul Toxicol Pharmacol 2018;94:183-96. https://doi.org/10.1016/j.yrtph.2018.01.022

[75] Li X, Chen L, Cheng F, Wu Z, Bian H, Xu C, Li W, Liu G, Shen X, Tang Y. In silico prediction of chemical acute oral toxicity using multi-classification methods. J Chem Inf Model 2014;54:1061-9. https://doi.org/10.1021/ci5000467

[76] Wai SK, Saiwan C, Idem R, Supap T, Nwaoha C. Carbon Dioxide (CO_2) Solubility in Diethylenetriamine and 2-Amino-2-Methyl-1-Proponal (DETA–AMP) Solvent System for Amine–Based CO_2 Capture in Flue Gas from Coal Combustion. Energy Procedia 2017;114: 1973-9. https://doi.org/10.1016/j.egypro.2017.03.1329

[77] Ramezani R, Mazinani S, Di Felice R. Density, Viscosity, pH, Heat of Absorption, and CO_2 Loading Capacity of Methyldiethanolamine and Potassium Lysinate Blend Solutions. J Chem Eng Data 2021;66:1611-29. https://doi.org/10.1021/acs.jced.0c00855

[78] Ahmed RE, Wiheeb AD. Enhancement of carbon dioxide absorption into aqueous potassium carbonate by adding amino acid salts. Mater Today: Proc 2020;20:611-6. https://doi.org/10.1016/j.matpr.2019.09.198

[79] Pandey D, Mondal MK. Experimental data and modeling for density and viscosity of carbon dioxide (CO_2)-loaded and-unloaded aqueous blend of 2-(ethylamino) ethanol (EAE) and aminoethylethanolamine (AEEA) for post-combustion CO_2 capture. J Mol Liq. 2021;330: 115678. https://doi.org/10.1016/j.molliq.2021.115678

[80] Shen S, Yang YN, Wang Y, Ren S, Han J, Chen A. CO_2 absorption into aqueous potassium salts of lysine and proline: density, viscosity and solubility of CO_2. Fluid Ph Equilibria 2015;399: 40-9. https://doi.org/10.1016/j.fluid.2015.04.021

[81] Sobrino M, Concepción EI, Gómez-Hernández Á, Martín MC, Segovia JJ. Viscosity and density measurements of aqueous amines at high pressures: MDEA-water and MEA-water mixtures for CO_2 capture. J Chem Thermodyn 2016;98:231-41. https://doi.org/10.1016/j.jct.2016.03.021

[82] Hsu CH, Li MH. Densities of aqueous blended amines. J Chem Eng Data 1997;42:502-7. https://doi.org/10.1021/je960356j

[83] Böttinger W, Maiwald M, Hasse H. Online NMR Spectroscopic Study of Species Distribution in MDEA−H_2O−CO_2 and MDEA−PIP−H_2O−CO_2. Ind Eng Chem Res 2008;47: 7917-26. https://doi.org/10.1021/ie800914m

[84] Kortunov PV, Siskin M, Baugh LS, Calabro DC. In situ nuclear magnetic resonance mechanistic studies of carbon dioxide reactions with liquid amines in aqueous systems: New insights on carbon capture reaction pathways. Energy Fuels 2015;29:5919-39. https://doi.org/10.1021/acs.energyfuels.5b00850

[85] Guo C, Chen S, Zhang Y. A ^{13}C NMR study of carbon dioxide absorption and desorption in pure and blended 2-(2-aminoethylamine) ethanol (AEEA) and 2-amino-2-

methyl-1-propanol (AMP) solutions. Int J Greenh Gas Control 2014;28:88-95. https://doi.org/10.1016/j.ijggc.2014.06.025

[86] Agnihotri N, Mondal MK. Comparison of non-catalytic and in-situ catalytic pyrolysis of Melia azedarach sawdust. J Anal Appl Pyrolysis. 2023;172:106006. https://doi.org/10.1016/j.jaap.2023.106006

[87] Nandiyanto AB, Oktiani R, Ragadhita R. How to read and interpret FTIR spectroscope of organic material. Indones J Sci Technol 2019;4:97-118. https://doi.org/10.17509/ijost.v4i1.15806

[88] Gao G, Li X, Jiang W, Zhao Z, Xu Y, Wu F, Luo C, Zhang L. Improved quasi-cycle capacity method based on microcalorimetry strategy for the fast screening of amino acid salt absorbents for CO_2 capture. Sep Purif Technol. 2022;289:120767. https://doi.org/10.1016/j.seppur.2022.120767

[89] Xiao M, Cui D, Liu H, Tontiwachwuthikul P, Liang Z. A new model for correlation and prediction of equilibrium CO_2 solubility in N-methyl-4-piperidinol solvent. AIChE J 2017;63: 3395-403. https://doi.org/10.1002/aic.15709

[90] Xie Q, Aroonwilas A, Veawab A. Measurement of heat of CO_2 absorption into 2-amino-2-methyl-1-propanol (AMP)/piperazine (PZ) blends using differential reaction calorimeter. Energy Procedia 2013;37:826-33. https://doi.org/10.1016/j.egypro.2013.05.175

[91] Mathias PM, O'Connell JP. The Gibbs–Helmholtz equation and the thermodynamic consistency of chemical absorption data. Ind Eng Chem Res 2012;51:5090-7. https://doi.org/10.1021/ie202668k

[92] Rochelle G, Chen E, Freeman S, Van Wagener D, Xu Q, Voice A. Aqueous piperazine as the new standard for CO_2 capture technology. Chem Eng J 2011;171:725-33. https://doi.org/10.1016/j.cej.2011.02.011

[93] Rho SW, Yoo KP, Lee JS, Nam SC, Son JE, Min BM. Solubility of CO_2 in aqueous methyldiethanolamine solutions. J Chem Eng Data 1997;42:1161-4. https://doi.org/10.1021/je970097d

[94] Elmobarak WF, Almomani F, Tawalbeh M, Al-Othman A, Martis R, Rasool K. Current status of CO_2 capture with ionic liquids: Development and progress. Fuel. 2023;344:128102. https://doi.org/10.1016/j.fuel.2023.128102

[95] Shao R, Stangeland A. Amines used in CO_2 capture-health and environmental impacts. Bellona report 2009;49:1-49.

[96] Hamm J, Allen D, Ceger P, Flint T, Lowit A, O'Dell L, Tao J, Kleinstreuer N. Performance of the GHS mixtures equation for predicting acute oral toxicity. Regul Toxicol Pharmacol. 2021;125:105007. https://doi.org/10.1016/j.yrtph.2021.105007

[97] Rey A, Gouedard C, Ledirac N, Cohen M, Dugay J, Vial J, Pichon V, Bertomeu L, Picq D, Bontemps D, Chopin F. Amine degradation in CO_2 capture. 2. New degradation products of MEA. Pyrazine and alkylpyrazines: analysis, mechanism of formation and toxicity. Int J Greenh Gas Control 2013;19:576-83. https://doi.org/10.1016/j.ijggc.2013.10.018

[98] Ramezani R, Mazinani S, Di Felice R. State-of-the-art of CO_2 capture with amino acid salt solutions. Rev Chem Eng 2022;38:273-99. https://doi.org/10.1515/revce-2020-0012

[99] Caplow M. Kinetics of carbamate formation and breakdown. J Am Chem Soc 1968;90: 6795-803. https://doi.org/10.1021/ja01026a041

[100] Danckwerts PV. The reaction of CO_2 with ethanolamines. Chem Eng Sci 1979;34:443-6. https://doi.org/10.1016/0009-2509(79)85087-3

[101] Crooks JE, Donnellan JP. Kinetics and mechanism of the reaction between carbon dioxide and amines in aqueous solution. J Chem Soc Perkin Trans 2 1989:331-3. https://doi.org/10.1039/P29890000331

[102] Da Silva EF, Svendsen HF. Ab initio study of the reaction of carbamate formation from CO_2 and alkanolamines. Ind Eng Chem Res 2004;43:3413-8. https://doi.org/10.1021/ie030619k

[103] Donaldson TL, Nguyen YN. Carbon dioxide reaction kinetics and transport in aqueous amine membranes. Ind Eng Chem Fundam 1980;19:260-6. https://doi.org/10.1021/i160075a005

[104] Shen KP, Li MH. Solubility of carbon dioxide in aqueous mixtures of monoethanolamine with methyldiethanolamine. J Chem Eng Data 1992;37:96-100. https://doi.org/10.1021/je00005a025

[105] Aronu UE, Gondal S, Hessen ET, Haug-Warberg T, Hartono A, Hoff KA, Svendsen HF. Solubility of CO_2 in 15, 30, 45 and 60 mass% MEA from 40 to 120 C and model representation using the extended UNIQUAC framework. Chem Eng Sci 2011;66:6393-406. https://doi.org/10.1016/j.ces.2011.08.042

[106] Gao H, Wu Z, Liu H, Luo X, Liang Z. Experimental studies on the effect of tertiary amine promoters in aqueous monoethanolamine (MEA) solutions on the absorption/stripping performances in post-combustion CO_2 capture. Energy Fuels 2017;31:13883-91. https://doi.org/10.1021/acs.energyfuels.7b02390

[107] Tong D, Trusler JM, Maitland GC, Gibbins J, Fennell PS. Solubility of carbon dioxide in aqueous solution of monoethanolamine or 2-amino-2-methyl-1-propanol: Experimental measurements and modeling. Int J Greenh Gas Control 2012;6:37-47. https://doi.org/10.1016/j.ijggc.2011.11.005

[108] Lee JL, Otto FD, Mather AE. Equilibrium between carbon dioxide and aqueous monoethanolamine solutions. J Appl Chem Biotechnol 1976;26:541-9. https://doi.org/10.1002/jctb.5020260177

[109] Xiao M, Cui D, Liu H, Tontiwachwuthikul P, Liang Z. A new model for correlation and prediction of equilibrium CO_2 solubility in N-methyl-4-piperidinol solvent. AIChE J 2017;63: 3395-403. https://doi.org/10.1002/aic.15709

[110] Bajpai A, Mondal MK. Equilibrium solubility of CO_2 in aqueous mixtures of DEA and AEEA. J Chem Eng Data 2013;58:1490-5. https://doi.org/10.1021/je3011776

[111] Kumar S, Mondal MK. Equilibrium solubility of CO_2 in aqueous binary mixture of 2-(diethylamine) ethanol and 1, 6-hexamethyldiamine. Korean J Chem Eng 2018;35:1335-40. https://doi.org/10.1007/s11814-018-0044-6

[112] Kumar S, Padhan R, Mondal MK. Equilibrium solubility measurement and modeling of CO_2 absorption in aqueous blend of 2-(diethyl amino) ethanol and ethylenediamine. J Chem Eng Data 2020;65:523-31. https://doi.org/10.1021/acs.jced.9b00699

[113] Srisang W, Pouryousefi F, Osei PA, Decardi-Nelson B, Akachuku A, Tontiwachwuthikul P, Idem R. Evaluation of the heat duty of catalyst-aided amine-based post combustion CO_2 capture. Chem Eng Sci 2017;170:48-57. https://doi.org/10.1016/j.ces.2017.01.049

[114] Hartono A, Mba EO, Svendsen HF. Physical properties of partially CO_2 loaded aqueous monoethanolamine (MEA). J Chem Eng Data 2014;59:1808-16. https://doi.org/10.1021/je401081e

[115] Choubtashani S, Rashidi H. CO_2 capture process intensification of water-lean methyl diethanolamine-piperazine solvent: Experiments and response surface modeling. Energy. 2023;267:126447. https://doi.org/10.1016/j.energy.2022.126447

[116] Kortunov PV, Siskin M, Baugh LS, Calabro DC. In situ nuclear magnetic resonance mechanistic studies of carbon dioxide reactions with liquid amines in aqueous systems: New insights on carbon capture reaction pathways. Energy Fuels 2015;29:5919-39. https://doi.org/10.1021/acs.energyfuels.5b00850

[117] Wang W, Zheng K, Peng Z, Liu B, Jia X, Tian J. Exploiting proton masking to protect amino achieve efficient capture CO_2 by amino-acids deep eutectic solvents. Sep Purif Technol. 2022;299:121787. https://doi.org/10.1016/j.seppur.2022.121787

[118] Xu S, Wang YW, Otto FD, Mather AE. Kinetics of the reaction of carbon dioxide with 2-amino-2-methyl-1-propanol solutions, Chem Eng Sci 1996;51:841-50. https://doi.org/10.1016/0009-2509(95)00327-4

[119] Amiri M, Shahhosseini S, Ghaemi A. Optimization of CO_2 capture process from simulated flue gas by dry regenerable alkali metal carbonate based adsorbent using response surface methodology. Energy Fuels 2017;31:5286-96. https://doi.org/10.1021/acs.energyfuels.6b03303

[120] Gilmour SG. Response surface designs for experiments in bioprocessing. Biometrics 2006;62:323-31. https://doi.org/10.1111/j.1541-0420.2005.00444.x

[121] Song C, Kitamura Y, Li S. Optimization of a novel cryogenic CO_2 capture process by response surface methodology (RSM). J Taiwan Inst Chem Eng 2014;45:1666-76. https://doi.org/10.1016/j.jtice.2013.12.009

[122] Gil MV, Martínez M, Garcia S, Rubiera F, Pis JJ, Pevida C. Response surface methodology as an efficient tool for optimizing carbon adsorbents for CO_2 capture. Fuel Process Technol 2013;106:55-61. https://doi.org/10.1016/j.fuproc.2012.06.018

[123] Saeidi M, Ghaemi A, Tahvildari K, Derakhshi P. Exploiting response surface methodology (RSM) as a novel approach for the optimization of carbon dioxide adsorption by dry sodium hydroxide. J Chin Chem Soc 2018;65:1465-75. https://doi.org/10.1002/jccs.201800012

[124] Tang Q, Lau YB, Hu S, Yan W, Yang Y, Chen T. Response surface methodology using Gaussian processes: Towards optimizing the trans-stilbene epoxidation over Co^{2+}–NaX catalysts. Chem Eng J 2010;156:423-31. https://doi.org/10.1016/j.cej.2009.11.002

[125] https://www.fishersci.com/store/msds?partNumber=AC126720010&productDescription=N-METHYLDIETHANOLAMINE%2C+1KG&vendorId=VN00032119&countryCode=US&language=en (accessed 09 November 2023).

[126] https://www.fishersci.com/store/msds?partNumber=AC115880050&productDescription=3-DIMETHYLAMINO-1-ROPANOL+5G&vendorId=VN00032119&countryCode=US&language=en (accessed 09 November 2023).

[127] Alliance Chemicals. https://www.alliancechemicals.com/wp-content/uploads/2019/01/ MEA- sds.pdf (accessed 09 November 2023).

[128] Ted Pella. https://www.tedpella.com/SDS_html/18315_sds.pdf (accessed 09 November 2023).

[129] Sigma-Aldrich. https://www.sigmaaldrich.com/IN/en/sds/aldrich/h11696 (accessed 09 November 2023).

[130] Spectrum. https://www.spectrumchemical.com/media/sds/AM156_AGHS.pdf (accessed 09 November 2023).

[131] Oxford Lab Fine. https://www.oxfordlabchem.com/msds/PIPERAZINE%20(Anhydrous). pdf (accessed 09 November 2023).

[132] Alliance Chemicals. https://www.alliancechemicals.com/wp-content/uploads/2011/10/DEA-sds.pdf (accessed 09 November 2023).

[133] North Metal and Chemical. https://northmetal.net/wp-content/uploads/Diethylaminoethanol-Diethylethanolamine-DEAE-DEEA-Pennad-150 C6H15NO-100-37-8-SDS.pdf (accessed 09 November 2023).

[134] Merck. https://www.sigmaaldrich.com/IN/en/sds/aldrich/471496 (accessed 09 November 2023).